Multimodal Ellipsoid Model for Non-Probabilistic Structural Uncertainty Quantification and Propagation

Jie Liu (liujie@hnu.edu.cn)
Hunan University https://orcid.org/0000-0003-3953-0693
Zhongbo Yu
Hunan University
Dequan Zhang
Hebei university of technology
Hao Liu
Hunan University

Original Article

Keywords: Multimodal ellipsoid model, Gaussian mixture model, Uncertainty quantification, Uncertainty propagation, Performance measure approach

Posted Date: June 22nd, 2020

DOI: https://doi.org/10.21203/rs.3.rs-37073/v1

Version of Record: A version of this preprint was published at International Journal of Mechanics and Materials in Design on June 4th, 2021. See the published version at https://doi.org/10.1007/s10999-021-09551-z.

Multimodal ellipsoid model for non-probabilistic structural uncertainty quantification and propagation

Jie Liu[*,1], Zhongbo Yu[1], Dequan Zhang[2], Hao Liu[1]

[1] State Key Laboratory of Advanced Design and Manufacturing for Vehicle Body, College of Mechanical and Vehicle Engineering, Hunan University, Changsha 410082, P. R. China

[2] State Key Laboratory of Reliability and Intelligence of Electrical Equipment, School of Mechanical Engineering, Hebei University of Technology, Tianjin 300401, P. R. China

* Corresponding author.

E-mail address: liujie@hnu.edu.cn (J. Liu)

* Other authors

yuzhongbo@hnu.edu.cn (Zhongbo Yu)

dequan.zhang@hebut.edu.cn (Dequan Zhang)

hao12.liu@midea.com (Hao Liu)

Abstract

The traditional ellipsoid convex set is a kind of basic non-probabilistic model to measure uncertainties. However, it is difficult or inaccurate to quantify the uncertainties of variables with multimodal distributed samples. In this paper, a more generalized non-probabilistic ellipsoid model named multimodal ellipsoid model is proposed to effectively deal with the multimodal distributed samples. The samples with one or more similar properties are clustered together, and the principal directions of the samples and characteristic matrix are appropriately found through the Gaussian mixture model. Then, the multimodal ellipsoid model can be constructed by using the elliptical contour features of the Gaussian model to measure the uncertainties of variables. The proposed multimodal ellipsoid model can not only establish traditional ellipsoid model, but also establish multi-ellipsoid model for uncertain variables with multimodal samples. Furthermore, combining with the multimodal ellipsoid model and performance measure approach, the uncertain propagation results of system are obtained accurately. Three numerical examples and one engineering application are provided to demonstrate the effectiveness and accuracy of the proposed multimodal ellipsoid model.

Keywords: Multimodal ellipsoid model; Gaussian mixture model; Uncertainty quantification; Uncertainty propagation; Performance measure approach

1. Introduction

There are various inherent uncertainties in practical structures, which are commonly associated with material properties, loads, manufacturing errors and boundary conditions, etc. To reasonably describe these uncertainties and analyze their influences on the structural performance is very important for reliability-based design (Chowdhury et al. 2009; Zhang et al. 2017; Zhang et al. 2020; Wei et al. 2020). At present, the probabilistic model is the most mature and frequently used measurement tool for structural uncertainties (Liu et al. 2015; Liu et al. 2018a; Du et al. 2000; Meng et al. 2017a; Wu et al. 2019). However, for some complex engineering problems, it is quite difficult to obtain sufficient samples and obtain accurate probability density function (PDF) of uncertain variables since the limitations of experimental conditions or cost. For this reason, many kinds of non-probabilistic methods have been developed to measure uncertainties, which include evidence theory (Cao et al. 2018; Cao et al. 2020; Li et al. 2016; Liu et al. 2020), probability-box (Ferson et al. 2002; Xiao et al. 2016; Chen et al. 2016), information theory (Klir. 2004), fuzzy sets (Dubois et al. 1989; Shi et al. 2018; Simoen et al. 2015), and convex model (Ben-Haim. 1994; Jiang et al. 2011; Zeng et al. 2018; Elishakoff et al. 2016; Truong et al. 2017).

As an effective supplement to the probabilistic model, Ref. (Ben-Haim. 1994) proposed a non-probabilistic convex model under the situation of limited samples, which has been gradually applied in academic and engineering fields. Generally, the non-probabilistic convex model is established based on the assumption that the uncertain parameters fall into a convex set. Interval model is an early-developed non-probabilistic convex model, which can be treated as a hypercube for multi-dimensional uncertain parameters (Du et al. 2005; Degrauwe et al. 2010). Obviously, the required information to construct such a hypercube model is only the upper and lower bounds of each uncertain variable, which is relatively easy to obtain in practical engineering. In the past two decades, a series of significant researches on the interval model (Moore. 1979; Jiang et al. 2007a; Pouresmaeeli et al. 2018) has been carried out. Ref. (Qiu et al. 2005a) proposed a parameter vertex solution algorithm to compute the lower and upper bounds of the structural eigenvalues due to the uncertain-but-bounded variables. Ref. (Kang et al. 2016) proposed a semi-definite programming (SDP) formulation method for construction of ellipsoid model. Ref. (Li et al. 2018) used the non-probabilistic interval model to describe uncertain parameters in model validation. Ref. (Jiang et al. 2007b; Jiang et al. 2008) suggested a series of uncertain optimization methods to solve the interval number programming

problem with uncertain variables in nonlinear objective functions and constraints. Ref. (Liu et al. 2018b) applied the interval model to the uncertain inverse problem to identify the dynamic loads acting on uncertain structures. Ref. (Meng et al. 2020) proposed an experimental data-driven exponential convex model for reliability assessment.

With the deepening and development of research, the correlation problem in uncertain variables gradually attracts many researchers' attentions. The interval model is limited to represent the correlations of uncertain parameters, because it can only provide the upper and lower bounds. In order to solve this problem, the ellipsoid model (Ben-Haim. 1994) was proposed and adopted in engineering as its ability to deal with variable correlation. Similar to the interval model, only the ellipsoid bound is required to construct an ellipsoid model, which can surround all the limited samples of uncertain variables, instead of their precise probability distribution. Further, the fluctuations of uncertain variables are assumed to fall into a single ellipsoidal domain. Many researches on how to construct the most suitable ellipsoidal convex model have been published. With the help of hypercube model, Ref. (Qiu et al. 2005b) proposed a modeling method to construct hyper ellipsoid with the minimum volume. And yet, as the axes of hypercube model are parallel to the axes of original coordinate system, the constructed hyper ellipsoid model for uncertain variables with different correlations possibly have a same spindle direction. Ref. (Zhu et al. 1996) applied the experimental samples to establish the ellipsoid model using the minimum volume, but the process was complicated. One most appropriate interval model was constructed, and then the minimal circumscribed ellipsoid was treated as an uncertainty measurement model. Ref. (Kumar et al. 2005) proposed an ellipsoid modeling method using experimental samples without the construction of hypercube. According to the different properties of variables, another ellipsoid convex model was proposed by Ref. (Kang et al. 2009). In addition, Ref. (Jiang et al. 2011) proposed a novel correlation analysis technique to construct multidimensional ellipsoid for uncertain structures. Ref. (Meng et al. 2018) created a mathematical foundation for non-probabilistic super parametric convex model to perform the reliability analysis and reliability-based design optimization. With the development of convex set theory, some related fields such as non-probabilistic uncertainty propagation (Qiu et al. 2003; Liu et al. 2018c) and uncertain topology optimization (Kang et al. 2009; Luo et al. 2009) have been gradually investigated. Based on the convex model, an uncertainty propagation algorithm was developed to compute the structural dynamic response bounds (Qiu et al. 2005). Using a quantified measure for non-

probabilistic reliability based on the ellipsoid convex model, a topology optimization of continuum structures (Luo et al. 2009) was investigated considering uncertain-but-bounded variables. Ref. (Meng et al. 2016) presented a decoupled strategy for non-probabilistic reliability-based design optimization to the efficiency. Ref. (Meng et al. 2017b) proposed a new directional stability transformation method for first order reliability analysis. Ref. (Wang et al. 2019) developed a non-probabilistic time-variant reliability-based optimization strategy for closed-loop controller design of vibration reduction issues.

Although the uncertainty modeling approaches based on the non-probabilistic convex set theory have achieved considerable developments, most of the above-mentioned ellipsoid models only use single convex model to surround the limited samples of uncertain variables as well as a lack of consideration regarding on the multimodal status of samples. Actually, the single ellipsoid model is only suitable for the situation that there is one simple peak of the distribution. However, in many instances, although the samples for establishing an ellipsoid convex model would be pretty limited, their distributions may have multiple distinct separate or intersecting multimodal. The multimodal situation is similar to the multi-peak situation of PDF in the probability theory (Zhang et al. 2019; Meng et al. 2020). Obviously, the traditional single ellipsoid model is not suitable for practically descript the multimodal of samples. More importantly, in such case, if the single ellipsoid model is still adapted to surround the samples with multimodal situation and quantify the uncertainty, the established ellipsoid domain will be relatively large and the corresponding uncertainty analysis or design results would be conservative. In order to establish a more reasonable ellipsoid model for the uncertain variables with single or multimodal, a novel multimodal ellipsoid model (MEM) is proposed in this study through the multimodal analysis based on Gaussian mixture model (GMM). For the non-probabilistic convex model to measure the variables' uncertainties with limited samples, the determination of the appropriate bounder of non-probabilistic model to surround the samples is primary. Although the GMM is commonly applied to model the probabilistic uncertainties, here even if the samples are limited, it still can be adopted to find the principal directions of the samples and it is beneficial to obtain the characteristic matrix of the non-probabilistic ellipsoid model for appropriately surrounding the samples. Meanwhile, the proposed MEM is a more generalized non-probabilistic ellipsoid model for uncertainty measurement, which can not only realize the traditional single ellipsoid modeling, but also can effectively establish a multi-ellipsoid for the uncertain

variables with multimodal samples.

In this paper, according to the inherent characteristics of uncertain variables' samples, the single or multimodal sample with similar property are gathered through Gaussian mixture model. For each cluster, the corresponding MEM can be established by using the compact elliptical contour feature of the Gaussian mixture model. Furthermore, combining the proposed MEM and performance measure approach (PMA) (Tu et al. 1999), an efficient and accurate uncertainty propagation method is proposed. The rest of this paper is organized as follows. In Section 2, two kinds of existing ellipsoid modeling methods are simply introduced. In Section 3, the proposed MEM is established based on the GMM and the ellipsoidal contour feature of the Gaussian mixture model. In Section 4, an efficient uncertainty propagation method based on the MEM and PMA is proposed. Section 5 presents three numerical examples and one engineering application to demonstrate the effectiveness of the proposed MEM and corresponding uncertainty propagation method. Some conclusions are summarized in Section 6.

2. Traditional ellipsoid model

Ellipsoid model is one of the most widely used non-probabilistic convex models for uncertainty measurement, in which the variations of uncertain variables are assumed to fall into an ellipsoidal convex set. During the modeling process of ellipsoid, the minimum volume of model is commonly adopted for most convex models. At present, the minimum volume optimization method (Zhu et al. 1996) and the correlation approximation method (Jiang et al. 2011) are two kinds of frequently-used ellipsoid modeling methods. Generally speaking, the minimum volume optimization method is used to search an ellipsoid with the minimum volume which can surround all the samples of uncertain variables, and the correlation approximation method is used to search a minimum volume ellipsoid for a given interval of uncertain variables.

2.1 Minimum volume optimization method

For n-dimensional uncertain variables $\mathbf{X}=[X_1, X_2, \mathrm{K}, X_n]^{\mathrm{T}}$, assume that there exists m experimental samples $\mathbf{X}^{(r)}, r=1,2,\cdots,m$ in the n-dimensional space. In order to measure the uncertainties, an ellipsoid model surrounding all the samples can be established as (Zhu et al. 1996),

$$E_X=\left\{\mathbf{X}\left|\left(\mathbf{X}-\mathbf{X}^{\mathrm{C}}\right)^{\mathrm{T}}\boldsymbol{\Omega}\left(\mathbf{X}-\mathbf{X}^{\mathrm{C}}\right)\le 1,\ \mathbf{X}\in \mathrm{R}^n\right.\right\} \tag{1}$$

where E_X denotes the ellipsoid domain of the uncertain variables $\mathbf{X}$. The superscripts C and T

represent the midpoint of ellipsoid domain and the transpose of a matrix, respectively. $\mathbf{\Omega}$ is a characteristic matrix of the *n*-dimensional ellipsoid model, which is a symmetric positive definite matrix as

$$\mathbf{\Omega} = \begin{bmatrix} g_{11} & g_{12} & \mathrm{L} & g_{1n} \\ g_{21} & g_{22} & \mathrm{L} & g_{2n} \\ \mathrm{M} & \mathrm{M} & & \mathrm{M} \\ g_{n1} & g_{n2} & \mathrm{L} & g_{nn} \end{bmatrix} \tag{2}$$

Here, Eq. (2) can determine the size and shape of the *n*-dimensional ellipsoid. As shown in Eq. (1), once the midpoint of ellipsoid domain $\mathbf{X}^{\mathrm{C}}$ and the characteristic matrix $\mathbf{\Omega}$ are determined, then the ellipsoid model can be obtained to measure the uncertainties of variables. Actually, it seems that there exist plenty of ellipsoids can be used to surround these *m* samples. However, the ellipsoid with a minimum volume is considered as the most appropriate one. Theoretically, such an ellipsoid model can be obtained by solving the following optimization problem,

$$\begin{cases} \min \prod_{i=1}^{n} \lambda_i \left(g_{11}, g_{12}, \cdots, g_{nn} \right) \\ \text{s.t. } \left(\mathbf{X}^{(r)} - \mathbf{X}^{\mathrm{C}} \right)^{\mathrm{T}} \begin{bmatrix} g_{11} & g_{12} & \mathrm{L} & g_{1n} \\ g_{21} & g_{22} & \mathrm{L} & g_{2n} \\ \mathrm{M} & \mathrm{M} & & \mathrm{M} \\ g_{n1} & g_{n2} & \mathrm{L} & g_{nn} \end{bmatrix} \left(\mathbf{X}^{(r)} - \mathbf{X}^{\mathrm{C}} \right) \le 1, \quad r = 1, 2, \cdots, m \\ \lambda_i \ge 0, \ i = 1, 2, \cdots, n \end{cases} \tag{3}$$

where λ_i denotes the half-length of the *i*th axis of the ellipsoid. It can be obtained through the eigenvalue decomposition of the characteristic matrix $\mathbf{\Omega}$, and the volume of the ellipsoid can be represented by the product of all the λ_i. The optimization variables of the above problem are all the elements g_{ij} in the characteristic matrix $\mathbf{\Omega}$ and the midpoint X_i^{C}. Unfortunately, if the dimension of uncertain variables and sample numbers are large enough, it seems hard to establish a minimum volume model (MVM) for uncertain variables.

2.2 Correlation approximation method

The basic idea of the correlation approximation method (CAM) (Jiang et al. 2011) is to establish a minimum volume ellipsoid to surround the samples for a given hypercube of uncertain variables. Different with the minimum volume optimization method, the CAM is defined as searching an ellipsoid in each two-dimensional sub-space. This ellipsoid should have two characteristics. (1) Ellipsoid and uncertain variables should be tangent. (2) Ellipsoid has a minimum volume in the

premise of first characteristic. These two characteristics can be guaranteed through the correlation model reported in Ref. (Jiang et al. 2011). Then, all the ellipsoids, which are established in two-dimensional sub-space, are assembled together in *n*-dimension space.

For the convenience of expression, firstly the uncertainty modeling problem with two-dimensional variables is discussed. Assume that all the possible values of X_1 and X_2 located in the marginal interval $\mathbf{X}^{\mathrm{I}}=\left[\mathbf{X}^{\mathrm{L}},\mathbf{X}^{\mathrm{U}}\right]$, where the superscripts I, L and U represent the interval, lower bound and upper bound, respectively. And the midpoint X_i^{C} and radius X_i^{W} of the interval are defined as,

$$\begin{cases} X_i^{\mathrm{C}}=\dfrac{X_i^{\mathrm{U}}+X_i^{\mathrm{L}}}{2} \\ X_i^{\mathrm{W}}=\sqrt{D\left(X_i\right)}=\dfrac{X_i^{\mathrm{U}}-X_i^{\mathrm{L}}}{2} \end{cases} \quad i=1,2 \tag{4}$$

where $D\left(X_i\right)$ is the defined variance which represents the deviation degree of uncertain parameter from midpoint. Further, the covariance $\mathrm{Cov}\left(X_1,X_2\right)$ and non-probabilistic correlation coefficient $\rho\left(X_1,X_2\right)$ of uncertain variables are defined as,

$$\begin{cases} \mathrm{Cov}\left(X_1,X_2\right)=\left(\lambda_1^2-\lambda_2^2\right)\sin\theta\cos\theta \\ \rho\left(X_1,X_2\right)=\dfrac{\mathrm{Cov}\left(X_1,X_2\right)}{\sqrt{D\left(X_1\right)}\sqrt{D\left(X_2\right)}} \end{cases} \tag{5}$$

where $\theta\left(-45^o\le\theta\le 45^o\right)$ is the rotation angle of the ellipse in the normal coordinate system. Therefore, the characteristic matrix $\mathbf{\Omega}$ of the ellipsoid model can be obtained through the inverse operation of the covariance matrix $\mathbf{\Sigma}$ of uncertain variables,

$$\mathbf{\Omega}=\mathbf{\Sigma}^{-1}=\begin{bmatrix} D\left(X_1\right) & \mathrm{Cov}\left(X_1,X_2\right) \\ sym. & D\left(X_2\right) \end{bmatrix}^{-1} \tag{6}$$

For an *n*-dimensional uncertain problem, the multi-dimensional ellipsoid can be established by assembling any two-dimensional ellipsoid model as the above-mentioned. For more details on the correlated ellipsoid model, one can refer to (Jiang et al. 2011).

In Eq. (6), the non-probabilistic correlation coefficient $\rho\left(X_1,X_2\right)$ or rotation angle θ needs to be determined to establish the ellipsoid model. Similar to Eq. (3), minimizing the area of the inscribed ellipse in the region of the two-dimensional marginal intervals can be applied to obtain a suitable rotation angle and the corresponding correlation coefficient. Fortunately, this optimization process

avoids the shortcomings of the minimum volume optimization method as the above-mentioned. Through the CAM, the high dimensional optimization problem is transformed into a series of two-dimensional optimization problems, which greatly simplifies the optimization process. Meanwhile, in the two-dimensional space, the optimization variable is only the correlation coefficient or rotation angle, and this is beneficial to ensure the positive definite property of ellipsoidal characteristic matrix during each optimization iteration. However, there are also some disadvantages in the CAM. Since the central point of ellipsoid model is previously specified as the midpoint of interval model, the established ellipsoid model is probably not the one with the minimum volume. Additionally, a few number of samples may be outside the established ellipsoid model (Jiang et al. 2011).

3. The proposed Multimodal ellipsoid model

As the above-mentioned, the two traditional ellipsoid modeling methods have the ability to achieve the uncertainty measurement of uncertain variables, but they do not fully consider the distribution and clustering status of the samples. In general, the number of samples to establish the non-probabilistic uncertainty measurement model is limited, but for many cases, the sample distribution still may display an obvious multimodal phenomenon, which is quite similar to the special PDF with multi-peak feature in the probability theory. Obvious, for such cases, these two above-mentioned ellipsoid modeling methods are not entirely suitable, as they can only establish a single ellipsoid model to surround the samples of uncertain variables. In order to effectively deal with various sample distributions, a more generalized ellipsoid model, namely MEM, based on cluster and GMM will be proposed in this section. The samples of uncertain variables are analyzed by using the GMM and then a single or multimodal samples can be obtained according to the distribution and clustering status of samples. Then, an appropriate elliptical contour lines are derived from the GMM to form the ellipsoid for surrounding all the samples.

3.1 Multimodal analysis for the samples of uncertain variables

Multimodal analysis belongs to the category of unsupervised machine learning method (Hofmann et al. 2011), which is developed to determine the multimodal of the samples (Fraley et al. 1998). It has been widely applied for data analysis in various fields. Usually, the pattern feature of samples is constructed to analyze the similarity between samples in multimodal analysis. The traditional pattern feature is a function with respect to distance, such as Block distance, Euclidean distance, Minkowski distance, which means each sample is assigned to a different cluster according to the distance between

samples and the given center point of each cluster (Kanungo et al. 2002). Another important pattern feature can be represented by a mathematical model about probability distribution model. Its purpose is to achieve the optimal matching between the samples and probability distribution model through fitting method (Celeux et al. 1995; Mcnicholas et al. 2008). In this section, the Gaussian clustering method will be introduced to realize the determinations of the principal directions of the samples and the characteristic matrix of the non-probabilistic multi-ellipsoid model.

3.1.1 Gaussian clustering

Gaussian clustering model is also called as GMM, which is a powerful framework for clustering analysis (Deng et al. 2013). Through observation, we find that the characteristic matrix of the ellipsoid model in Eq. (6) has the same formula with exponential term of the GMM, so it is promising to introduce it for the ellipsoid modeling. Even if the samples are limited, when the samples are shown the obvious multimodal, the advantages of the GMM still can be utilized to reasonably obtain the principal directions of the samples and to properly construct a non-probabilistic single or multiple ellipsoid model. When the samples are limited and the distribution of samples appears to one or more multimodal, one or more Gaussian functions (Fraley et al. 1998) can be adopted to descript their distribution as follows

$$f\left(\mathbf{X}|\partial\right)=\sum_{k=1}^{K}\alpha_k\Phi\left(\mathbf{X}|\boldsymbol{\mu}_k,\boldsymbol{\Sigma}_k\right) \tag{7}$$

where $\partial=\left(\alpha_1,\mathrm{L}\ ,\alpha_K,\mu_1,\mathrm{L}\ ,\mu_K,\Sigma_1,\mathrm{L}\ ,\Sigma_K\right)$ denotes the characteristic parameters of the GMM, $f\left(\mathbf{X}|\partial\right)$ is the Gaussian function for uncertain variables $\mathbf{X}$ with parameters ∂, K is a cluster number, α_k ($0<\alpha_k<1$ and $\sum_{k=1}^{K}\alpha_k=1$) is the weighted value or mixture ratio of the kth cluster, and $\Phi\left(\mathbf{X}|\boldsymbol{\mu}_k,\boldsymbol{\Sigma}_k\right)$ denotes the Gaussian function with mean vector $\boldsymbol{\mu}_k$ and covariance matrix $\boldsymbol{\Sigma}_k$ for the kth cluster. For the non-probabilistic convex model to measure the variables' uncertainties with limited samples, in fact, the distribution of the samples is unconcerned, and the focus is to determine the appropriate convex bounder to compactly surround the samples. Therefore, although the GMM is less accurate to descript their distribution under the limited samples, it still can be utilized to find the principal directions of the samples, especially for the situation that the samples exist multimodal. And the determined the principal directions by GMM will form the foundation to establish the appropriate

ellipsoid model.

For the GMM in Eq. (7), $3K$ unknown parameters ∂ can be determined by the maximum likelihood estimation (MLE) method. Assume that all the samples of uncertain variables $\mathbf{X}^{(r)}, r=1,2,\mathrm{L}\ ,m$ are independent, and then the probability of the event $\xi_X=\left\{\mathbf{X}^{(1)},\mathbf{X}^{(2)},\cdots,\mathbf{X}^{(m)}\right\}$ with parameters ∂ is formulated as

$$P\left(\xi_X|\partial\right)=\prod_{r=1}^{m}f\left(\mathbf{X}^{(r)}|\partial\right) \tag{8}$$

Then, in order to obtain the optimal values of parameters ∂, the following optimization problem based on the MLE is built,

$$\begin{cases}\max\limits_{\partial}\ L(\partial)=\ln\left(P\left(\xi_X|\partial\right)\right)=\sum\limits_{r=1}^{m}\ln\left(\sum\limits_{k=1}^{K}\alpha_k\Phi\left(X^{(r)}|\boldsymbol{\mu}_k,\boldsymbol{\Sigma}_k\right)\right)\\ \text{s.t.}\ \ \sum\limits_{k=1}^{K}\alpha_k=1,\ \ 0<\alpha_k<1\end{cases} \tag{9}$$

where $L(\partial)$ is the likelihood function of the event ξ_X. As the number of parameters to be estimated may be large, an efficient expectation-maximization (EM) algorithm (Dempster et al. 1997) is adopted.

3.1.2 Expectation-maximization algorithm for the GMM

The EM algorithm mainly consists of two steps, i.e. E-step and M-step, which is a general approach to implement the MLE effectively. The key of the EM algorithm is Jensen's inequality (Kass. 1990), and the Lemma about Jensen's inequality is introduced as follow.

Lemma. If function $f(\cdot)$ is a convex function on its actual definition domain, it should satisfy the Jensen's inequality $\mathrm{E}\left[f\left(x\right)\right]\geq f\left(\mathrm{E}\left[x\right]\right)$. Obviously, if function $f(\cdot)$ is a concave function, it should satisfy the inequality $\mathrm{E}\left[f\left(x\right)\right]\leq f\left(\mathrm{E}\left[x\right]\right)$, in which E[·] denotes the expectation function of independent variable x.

(1) **E-step**

The aim of E-step is to construct the expectation of likelihood function $L(\partial)$. The estimated conditional probability of uncertain variables $\mathbf{X}^{(r)}$ from the kth component can be expressed as,

$$\beta_k\left(\mathbf{X}^{(r)}\right)=\frac{\hat{\alpha}_k\Phi\left(\mathbf{X}^{(r)}\middle|\hat{\mu}_k,\hat{\Sigma}_k\right)}{\sum_{j=1}^{K}\hat{\alpha}_j\Phi\left(\mathbf{X}^{(r)}\middle|\hat{\mu}_j,\hat{\Sigma}_j\right)},\quad r=1,2,\mathrm{L}\ ,m;\ \ k=1,2,\mathrm{L}\ ,K \tag{10}$$

where $\beta_k\left(\mathbf{X}^{(r)}\right)$ denotes the conditional probability. $\hat{\alpha}$, $\hat{\boldsymbol{\Sigma}}$ and $\hat{\boldsymbol{\mu}}$ represent the estimated parameters. Then, combing with the Jensen's inequality and the concave character of likelihood function, we can obtain the following likelihood function formula,

$$\begin{aligned}L(\partial)&=\sum_{r=1}^{m}\ln\sum_{k=1}^{K}\alpha_k\Phi\left(\mathbf{X}^{(r)}\middle|\mu_k,\Sigma_k\right)\\&=\sum_{r=1}^{m}\ln\sum_{k=1}^{K}\beta_k\left(\mathbf{X}^{(r)}\right)\frac{\alpha_k\Phi\left(\mathbf{X}^{(r)}\middle|\mu_k,\Sigma_k\right)}{\beta_k\left(\mathbf{X}^{(r)}\right)}\\&\geq\sum_{r=1}^{m}\sum_{k=1}^{K}\beta_k\left(\mathbf{X}^{(r)}\right)\ln\frac{\alpha_k\Phi\left(\mathbf{X}^{(r)}\middle|\mu_k,\Sigma_k\right)}{\beta_k\left(\mathbf{X}^{(r)}\right)}\end{aligned} \tag{11}$$

The essence of Eq. (11) is the expectation function of the conditional probability $\beta_k\left(\mathbf{X}^{(r)}\right)$.

(2) **M-step**

The aim of M-step is to calculate the lower bound of $L(\partial)$, which is the maximum expectation. Based on the MLE, once the likelihood function $L(\partial)$ is equal to the maximum expectation in Eq. (11), the corresponding parameters $\hat{\partial}=\left(\hat{\alpha}_1,\mathrm{L}\ ,\hat{\alpha}_K,\hat{\mu}_1,\mathrm{L}\ ,\hat{\mu}_K,\hat{\boldsymbol{\Sigma}}_1,\mathrm{L}\ ,\hat{\boldsymbol{\Sigma}}_K\right)$ can be treated as the optimal values of GMM,

$$L\left(\hat{\partial}\right)=\sum_{r=1}^{m}\sum_{k=1}^{K}\beta_k\left(\mathbf{X}^{(r)}\right)\ln\frac{\alpha_k\Phi\left(\mathbf{X}^{(r)}\middle|\boldsymbol{\mu}_k,\boldsymbol{\Sigma}_k\right)}{\beta_k\left(\mathbf{X}^{(r)}\right)} \tag{12}$$

Considering the necessary condition of the extreme value theorem and the constraint conditions $\sum_{k=1}^{K}\alpha_k=1$, make the partial derivatives of Eq. (12) with respect to the parameters α_k, $\boldsymbol{\mu}_k$ and $\boldsymbol{\Sigma}_k$ equal to zero. Then, the optimal estimation of the parameters of the GMM can be obtained as follows,

$$\begin{cases} \alpha_k = \dfrac{\sum_{r=1}^{m} \beta_k\left(\mathbf{X}^{(r)}\right)}{m} \\ \boldsymbol{\mu}_k = \dfrac{\sum_{r=1}^{m} \beta_k\left(\mathbf{X}^{(r)}\right)\mathbf{X}^{(r)}}{\sum_{r=1}^{m} \beta_k\left(\mathbf{X}^{(r)}\right)} \\ \boldsymbol{\Sigma}_k = \dfrac{\sum_{r=1}^{m} \beta_k\left(\mathbf{X}^{(r)}\right)\left(\mathbf{X}^{(r)}-\boldsymbol{\mu}_k\right)^{\mathrm{T}}\left(\mathbf{X}^{(r)}-\boldsymbol{\mu}_k\right)}{\sum_{r=1}^{m} \beta_k\left(\mathbf{X}^{(r)}\right)} \end{cases} \tag{13}$$

To sum up, the EM algorithm can refine partitions when started sufficiently close to the optimal value, which are the maximum likelihood estimation of the characteristic parameters of GMM on Eq. (7), by E-step of Eq. (11) and M-step of Eq. (13). The established GMM according to the samples of uncertain variables will be used to construct the proposed MEM in the next section.

3.2 Multimodal ellipsoid modeling

As each sub-item of the GMM in Eq. (7) indicates a sample cluster with the similar distribution feature for uncertain variables, the corresponding multi-ellipsoid model for uncertainty measurement can be derived from each Gaussian sub-model to surround the samples fallen in the same cluster. In this way, a single ellipsoid or multi-ellipsoid model can be reasonably constructed according to the determined the principal directions and characteristic matrix by GMM.

3.2.1 Single-MEM

When all the samples of *n*-dimensional uncertain variables only display one cluster, the GMM can be simply expressed as,

$$f\left(\mathbf{X}|\partial\right)=\Phi\left(\mathbf{X}|\boldsymbol{\mu},\boldsymbol{\Sigma}\right)=\left(2\pi\right)^{-n/2}\left|\boldsymbol{\Sigma}\right|^{-1/2}\exp\left(-\frac{1}{2}\left(\mathbf{X}-\boldsymbol{\mu}\right)^{\mathrm{T}}\boldsymbol{\Sigma}^{-1}\left(\mathbf{X}-\boldsymbol{\mu}\right)\right) \tag{14}$$

in Eq. (14), $\boldsymbol{\Sigma}$ is the covariance matrix and $|\boldsymbol{\Sigma}|$ denotes the determinant of $\boldsymbol{\Sigma}$. Parameters $\boldsymbol{\mu}$ and $\boldsymbol{\Sigma}$ of Gaussian model can be appropriately determined by clustering the samples based on the above-mentioned EM algorithm. As the characteristic matrix of the ellipsoid model has the same formula with exponential term of the GMM, to treat the parameters $\boldsymbol{\mu}$ and $\boldsymbol{\Sigma}$ as the center point and characteristic matrix of ellipsoid, the bounds of a series of ellipsoids with respect to the uncertain variables can be derived through the contour surface of Gaussian model,

$$t(\mathbf{X}) = (\mathbf{X}-\boldsymbol{\mu})^{\mathrm{T}} \boldsymbol{\Sigma}^{-1} (\mathbf{X}-\boldsymbol{\mu}) = R^2 \tag{15}$$

where R^2 denotes the scale ratio of the contour ellipsoid. The optimal $\hat{R}^2$ can be determined through the following steps

Step 1. Give an initial value of R and set a step size ΔR

Step 2. Generate the contour ellipsoid by using the current R

Step 3. If all the samples are enveloped by the current contour ellipsoid as Eq. (15), the current R is considered as the optimal R and $\hat{R}^2 = R^2$. Otherwise, $R = R + \Delta R$ and go back to Step 2.

Ensuring that all the samples can fall into the ellipsoid, and the corresponding single-MEM can be constructed as

$$E_X = \left\{ \mathbf{X} \middle| (\mathbf{X}-\boldsymbol{\mu})^{\mathrm{T}} \boldsymbol{\Sigma}^{-1} (\mathbf{X}-\boldsymbol{\mu}) \le \hat{R}^2 \right\} \tag{16}$$

Taking two-dimensional problem as example, the established single-MEM for uncertainty measurement and the corresponding GMM for clustering samples are shown in Fig. 1. It is indicated that the samples are compactly surrounded by the constructed MEM. More importantly, the correlation of the uncertain variables can also be properly considered through the principal directions of samples obtained by GMM. Meanwhile, the proposed MEM avoids the disadvantages of the minimum volume method, such as large computational efforts. And for the multi-dimensional problems, the corresponding MEM can also be conveniently constructed without decomposing it into multiple two-dimensional models as the CAM (Jiang et al. 2011).

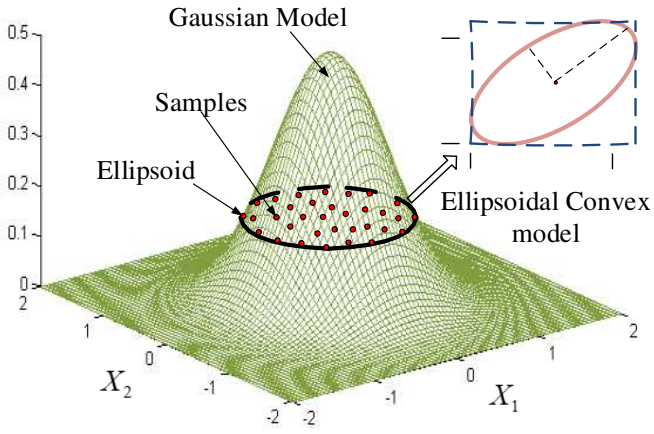

Fig.1 Single-peak distribution for two dimensional uncertain variables

3.2.2 Multi-MEM

The main disadvantage of the single ellipsoid model is that the intrinsic distribution status of

samples is ignored, and all the samples are simply surrounded by a single ellipsoid. Essentially, it is not appropriate to describe the uncertainty of variables with multimodal sample using the single ellipsoid. However, the proposed MEM can effectively analyze the samples with a similar distribution for establishing a more reasonable multi-ellipsoid model to measure the uncertainties of variables.

For the convenient expression, it can be assumed that all the samples of uncertain variables have two clusters. Then, the corresponding GMM built by the EM algorithm can be expressed as,

$$\begin{aligned} f(\mathbf{X}) = & \frac{\alpha_1}{(2\pi)^{n/2}|\mathbf{\Sigma}_1|^{1/2}} \exp\left(-\frac{1}{2}(\mathbf{X}-\boldsymbol{\mu}_1)^{\mathrm{T}}\mathbf{\Sigma}_1^{-1}(\mathbf{X}-\boldsymbol{\mu}_1)\right) \\ & + \frac{\alpha_2}{(2\pi)^{n/2}|\mathbf{\Sigma}_2|^{1/2}} \exp\left(-\frac{1}{2}(\mathbf{X}-\boldsymbol{\mu}_2)^{\mathrm{T}}\mathbf{\Sigma}_2^{-1}(\mathbf{X}-\boldsymbol{\mu}_2)\right) \end{aligned} \tag{17}$$

In Eq. (17), each sub-item is a single Gaussian ellipsoid model, and thus, a multi-MEM can be established by the union operation of these two single ellipsoids,

$$E_X = \left\{\mathbf{X}\middle|(\mathbf{X}-\boldsymbol{\mu}_1)^{\mathrm{T}}\mathbf{\Sigma}_1^{-1}(\mathbf{X}-\boldsymbol{\mu}_1) \le \hat{R}_1^2 \ \mathrm{U}\ (\mathbf{X}-\boldsymbol{\mu}_2)^{\mathrm{T}}\mathbf{\Sigma}_2^{-1}(\mathbf{X}-\boldsymbol{\mu}_2) \le \hat{R}_2^2\right\} \tag{18}$$

It can be ensured that the ellipsoids surround the relevant clustering samples through the appropriate scale ratios $\hat{R}_1^2$ and $\hat{R}_2^2$. Additionally, according to the sample distribution and the established GMM, there are two typical multi-MEMs. For the Type I, there is no intersection region for the single ellipsoids as shown in Fig. 2, while for the Type II, there exists an intersection region between these two ellipsoids as shown in Fig. 3.

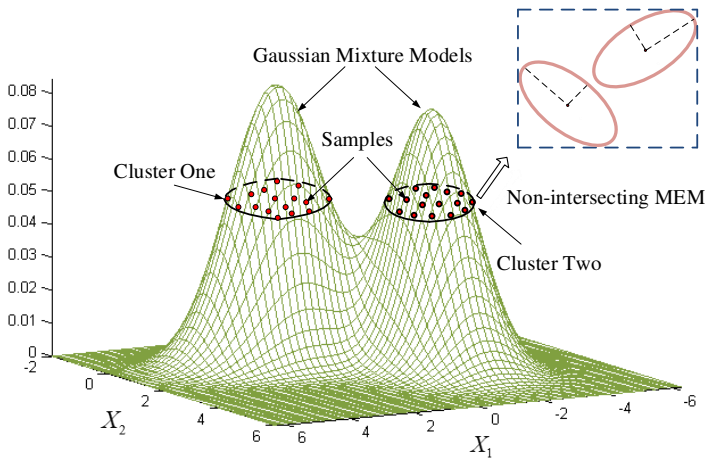

Fig.2 Type I: Non-intersecting MEM for two dimensional uncertain variables

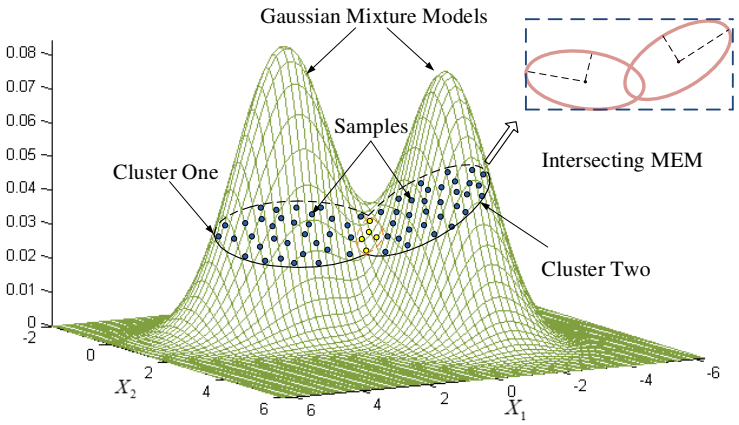

Fig.3 Type II: Intersecting MEM for two dimensional uncertain variables

4. Non-probabilistic uncertainty propagation

As the multi-MEM is the union of several single ellipsoid models, the uncertainty propagation method will be presented only for the single ellipsoid model. The system function of uncertainty propagation can be expressed as,

$$\begin{cases} y = z(\mathbf{X}) \\ \mathbf{X} \in E_X = \left\{ \mathbf{X} \middle| \left(\mathbf{X} - \mathbf{X}^{\mathrm{c}}\right)^{\mathrm{T}} \boldsymbol{\Omega} \left(\mathbf{X} - \mathbf{X}^{\mathrm{c}}\right) \le 1 \right\} \end{cases} \tag{19}$$

where y and $z(\cdot)$ denote the system response and system function.

Firstly, the space of uncertain variables (i.e. X space) is transformed into a set of regularized parameter space (i.e. U space),

$$U_i = \frac{X_i - X_i^{\mathrm{C}}}{X_i^{\mathrm{W}}},\ i = 1, 2, \cdots, n \tag{20}$$

Then the initial uncertain domain E_X can be transformed into a regularized convex domain E_U,

$$E_U = \left\{ \mathbf{U} \middle| \mathbf{U}^{\mathrm{T}} \boldsymbol{\Omega}_U \mathbf{U} \le 1 \right\} \tag{21}$$

where $\boldsymbol{\Omega}_U$ denotes a characteristic matrix of the transformed convex model in the U space.The eigenvalue decomposition is performed for the characteristic matrix,

$$\begin{cases} \mathbf{Q}^{\mathrm{T}} \boldsymbol{\Omega}_U \mathbf{Q} = \boldsymbol{\Lambda} \\ \mathbf{Q}^{\mathrm{T}} \mathbf{Q} = \mathbf{I} \end{cases} \tag{22}$$

where $\mathbf{Q}$ is an orthogonal matrix formed by the normalized eigenvectors, $\boldsymbol{\Lambda}$ is a diagonal matrix formed by the eigenvalues of $\boldsymbol{\Omega}_U$ and $\mathbf{I}$ is an identity matrix. Then another linear transformation is subsequently introduced,

$$\boldsymbol{\delta} = \boldsymbol{\Lambda}^{1/2}\mathbf{Q}^{\mathrm{T}}\mathbf{U} \tag{23}$$

By using Eq. (22) and (23), E_U can be further transformed into a unit sphere domain E_δ in the δ space,

$$E_\delta = \left\{\boldsymbol{\delta} \middle| \boldsymbol{\delta}^{\mathrm{T}}\boldsymbol{\delta} \le 1\right\} \tag{24}$$

Therefore, the corresponding system function in the δ space can be expressed as following,

$$Y = Z(\boldsymbol{\delta}) \tag{25}$$

where $Z(\cdot)$ denotes the system function in the δ space.

Assume that the degree of nonlinearity of system function is not high, and according to the linear programming theory (Jiang et al. 2008b), the optimal response of Eq. (21) will certainly occur on the boundary of the ellipsoid E_X (Wang et al. 2008). As the space transformation of uncertain variables is linear, obviously, the optimal response also occurs on the boundary of the ellipsoid E_δ in the δ space. For a two dimensional problem, the extreme state of system response in δ space is shown in Fig. 4, where δ_1^* and δ_2^* denotes the extreme value points in the δ space.

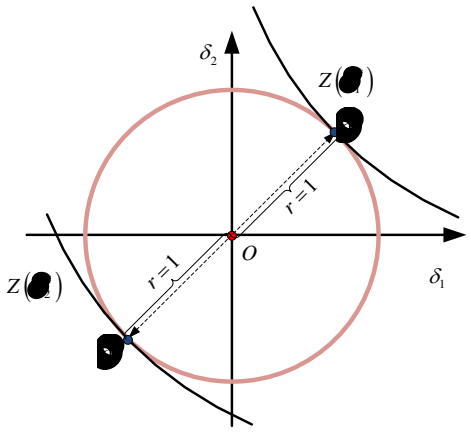

Fig.4 Extreme state of system response in unit sphere space

Then, the Lagrange-multiplier method (Kadapa et al. 2016) can be used to determine the analytic optimal solutions,

$$l = Z(\boldsymbol{\delta}) + \tau\left(\boldsymbol{\delta}^{\mathrm{T}}\boldsymbol{\delta} - 1\right) \tag{26}$$

where l and τ denote the Lagrange function and Lagrange multiplier, respectively. Considering the necessary condition of the extreme value theorem, the extreme value point of Eq. (26) can be obtained when the first order differential equation of l equals to zero, i.e.

$$\frac{\partial l}{\partial \boldsymbol{\delta}} = \nabla Z(\boldsymbol{\delta}) + 2\tau\boldsymbol{\delta} = 0 \tag{27}$$

$$\boldsymbol{\delta}^* = -\frac{\nabla Z\left(\boldsymbol{\delta}^*\right)}{2\tau} \tag{28}$$

where $\nabla Z(\cdot)$ denotes the partial derivative of system function in the δ space. Combining Eq. (28) and $E_\delta = \boldsymbol{\delta}^{\mathrm{T}}\boldsymbol{\delta} = 1$, the Lagrange multiplier τ can be obtained as,

$$\tau = \pm\frac{\sqrt{\nabla^{\mathrm{T}} Z(\boldsymbol{\delta})\nabla Z(\boldsymbol{\delta})}}{2} \tag{29}$$

$$\boldsymbol{\delta}^* = \mathrm{m}\frac{\nabla Z\left(\boldsymbol{\delta}^*\right)}{\left\|\nabla Z\left(\boldsymbol{\delta}^*\right)\right\|} \tag{30}$$

where $\|\cdot\|$ denotes the norm of a vector. In Eq. (30), it is clearly that the vector direction of extreme value point to origin point and the gradient direction are collinear. Hence, once the extreme value point is obtained in the δ space, the bounds of system response can be calculated by the inverse space transformation.

Performance measure approach is an effective method to calculate the most suitable limit-state function by giving a reliability index. As we know, the reliability index is the minimum distance from the origin to the limit-state function. To sum up, the space of uncertain variables transformed from the X space to the δ space, so the propagation process in the above section can be considered as the computation of corresponding most suitable limit-state function or the extreme value of system response as the precondition of a given reliability index. According to Ref. (Youn et al. 2004), the optimization model can be constructed as follows,

$$\begin{aligned} &\min \gamma = \cos^{-1}\frac{\boldsymbol{\delta}\cdot\nabla Z(\boldsymbol{\delta})}{\|\boldsymbol{\delta}\|\cdot\left\|\nabla Z(\boldsymbol{\delta})\right\|} \\ &s.t. \quad \boldsymbol{\delta}^{\mathrm{T}}\boldsymbol{\delta} = 1 \end{aligned} \tag{31}$$

where γ is the angle between δ and $\nabla Z(\boldsymbol{\delta})$. The optimization process is summarized in Fig. 5.

Step 1. Specify an initial point δ_i, and set $\mathbf{d}_i = \boldsymbol{\delta}_i$;

Step 2. Calculate the gradient $\nabla Z(\boldsymbol{\delta}_i)$;

Step 3. If $\gamma_i \le \varepsilon$, where ε is a small angle, then $\boldsymbol{\delta}^* = \boldsymbol{\delta}_i$. Otherwise, go to Step 4.

Step 4. Update the search direction $\mathbf{d}_{i+1} = \frac{\mathbf{d}_i}{\|\mathbf{d}_i\|} + \frac{\nabla Z(\boldsymbol{\delta}_i)}{\left\|\nabla Z(\boldsymbol{\delta}_i)\right\|}$ and the extreme point $\boldsymbol{\delta}_{i+1} = \frac{\mathbf{d}_{i+1}}{\|\mathbf{d}_{i+1}\|}$,

then go back to Step 2.

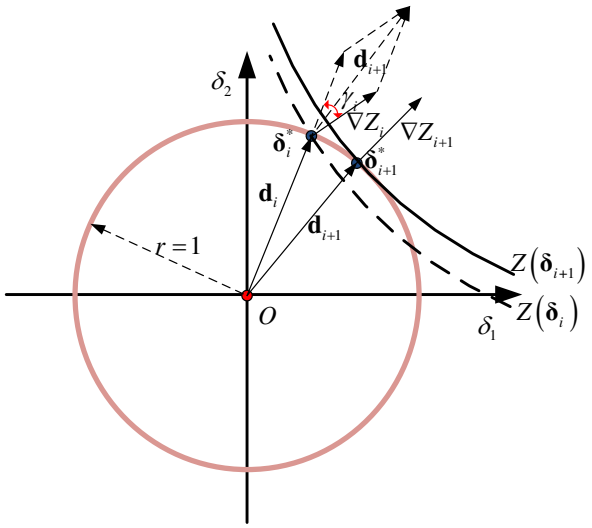

Fig.5 The updating of search direction in space

The uncertainty quantification and propagation procedure by MEM is summarized in Table 1

Table 1 Procedure of the uncertainty modeling and propagation by MEM

Uncertainty modeling procedure

Input: Samples of uncertain variables $\mathbf{X}^{(r)}, r=1,2,\mathrm{L}\ ,m$

Step 1. Apply GMM to construct the non-probabilistic ellipsoid model by Gaussian function . $f\left(\mathbf{X}|\partial\right)=\sum_{k=1}^{K}\alpha_k\Phi\left(\mathbf{X}|\boldsymbol{\mu}_k,\boldsymbol{\Sigma}_k\right)$.

Step 2. Construct the MLE functions $L(\partial)$ and substitute the samples into $L(\partial)$.

Step 3. Implement E-step to construct the expectation of likelihood functions by substituting the samples into MLE functions.

Step 4: Implement M-step to calculate the lower bound of $L(\partial)$. Then obtain the parameters $\hat{\partial}=\left(\hat{\alpha}_1,\mathrm{L}\ ,\hat{\alpha}_K,\hat{\mu}_1,\mathrm{L}\ ,\hat{\mu}_K,\hat{\boldsymbol{\Sigma}}_1,\mathrm{L}\ ,\hat{\boldsymbol{\Sigma}}_K\right)$ of the Gaussian function ;

Step 5: Based on GMM, determine each optimal R^2 of the contour ellipsoid that can envelop the clustered samples, and then obtain the multimodal ellipsoids;

Output: Multimodal ellipsoid $E_X=\left\{\mathbf{X}\left|\bigcup_{k=1}^{K}\left\{\left(\mathbf{X}-\boldsymbol{\mu}_k\right)^{\mathrm{T}}\boldsymbol{\Sigma}_k^{-1}\left(\mathbf{X}-\boldsymbol{\mu}_k\right)\le\hat{R}_k^2\right\}\right.\right\}$;

Uncertainty propagation procedure

Input: Multimodal ellipsoid E_X

Step 1: Transform the uncertain domain of E_X into regularized unit sphere domain $E_\delta = \left\{ \boldsymbol{\delta} \middle| \boldsymbol{\delta}^{\mathrm{T}} \boldsymbol{\delta} \le 1 \right\}$. And the transformed system function can be expressed as $Y = Z(\boldsymbol{\delta})$;

Step 2: Adopt Lagrange-multiplier method to determine the analytic optimal solutions $l = Z(\boldsymbol{\delta}) + \tau\left(\boldsymbol{\delta}^{\mathrm{T}} \boldsymbol{\delta} - 1\right)$;

Step 3: Differentiate l with respect to Z and let the differential equation equal to zero, yielding $\boldsymbol{\delta}^* = -\dfrac{\nabla Z(\boldsymbol{\delta}^*)}{2\tau}$;

Step 4: Construct the optimization problem

$$\min \gamma = \cos^{-1} \frac{\boldsymbol{\delta} \cdot \nabla Z(\boldsymbol{\delta})}{\|\boldsymbol{\delta}\| \cdot \|\nabla Z(\boldsymbol{\delta})\|}, \; s.t. \quad \boldsymbol{\delta}^{\mathrm{T}} \boldsymbol{\delta} = 1;$$

Step 5: Specify an initial point δ_i, and set $\mathbf{d}_i = \boldsymbol{\delta}_i$;

Step 6: Calculate the gradient $\nabla Z(\boldsymbol{\delta}_i)$;

Step 7: If $\gamma_i \le \varepsilon$, where ε is a small angle, then $\boldsymbol{\delta}^* = \boldsymbol{\delta}_i$. Otherwise, go back to Step 4. Update the search direction $\mathbf{d}_{i+1} = \dfrac{\mathbf{d}_i}{\|\mathbf{d}_i\|} + \dfrac{\nabla Z(\boldsymbol{\delta}_i)}{\|\nabla Z(\boldsymbol{\delta}_i)\|}$ and the extreme point $\boldsymbol{\delta}_{i+1} = \dfrac{\mathbf{d}_{i+1}}{\|\mathbf{d}_{i+1}\|}$, and then go back to Step 2;

Step 8: Calculate the maximum and minimum values of $Z(\boldsymbol{\delta}^*)$;

Step 9: Combine the propagated result under each ellipsoid and obtain the upper and lower bounds of the responses.

Output: Max / Min $Z(\boldsymbol{\delta}^*)$

5. Numerical examples and discussions

5.1 Numerical example 1

In this example, 39 samples of three independent uncertain variables $\mathbf{X} = [X_1, X_2, X_3]^{\mathrm{T}}$ are considered, the values of which are listed in Appendix. Firstly, the proposed MEM is applied to quantify the uncertain variables under these samples. The optimal parameters of the single MEM can

be obtained as follows,

$$\boldsymbol{\Sigma} = \begin{bmatrix} 1.9843 & 0.2139 & 0.3223 \\ 0.2139 & 0.8123 & 0.1132 \\ 0.3223 & 0.1132 & 0.2207 \end{bmatrix} \tag{32}$$

$$\boldsymbol{\mu} = \left[3.93, 4.01, 3.96\right]^{\mathrm{T}} \tag{33}$$

When $R^2 = 4.83$, we can obtain a critical contour ellipsoid, which can compactly surround all the samples of uncertain variables. Hence, the following single MEM can be established for appropriately surrounding the samples.

$$\begin{bmatrix} X_1 - 3.928 \\ X_2 - 4.012 \\ X_3 - 3.957 \end{bmatrix}^{\mathrm{T}} \begin{bmatrix} 1.9843 & 0.2139 & 0.3223 \\ 0.2139 & 0.8123 & 0.1132 \\ 0.3223 & 0.1132 & 0.2207 \end{bmatrix}^{-1} \begin{bmatrix} X_1 - 3.928 \\ X_2 - 4.012 \\ X_3 - 3.957 \end{bmatrix} \le 4.83 \tag{34}$$

In order to make a comparison, we can make normalization for the MEM in Eq. (34). And, the results are compared with the CAM, MVM and SDP, which are shown in Table 2 and Fig. 6. From the compared results, it can find that the established single MEM is closed to MVM and CAM, which indicates that the proposed uncertainty modeling method is effective. The SDP provides a smaller volume but some of the points may not be enveloped. Meanwhile, the modeling process of MEM based on maximum likelihood estimation is more convenient than SDP, MVM (optimization for all the parameters of characteristic matrix) and CAM (decomposition into several two dimensional optimizations).

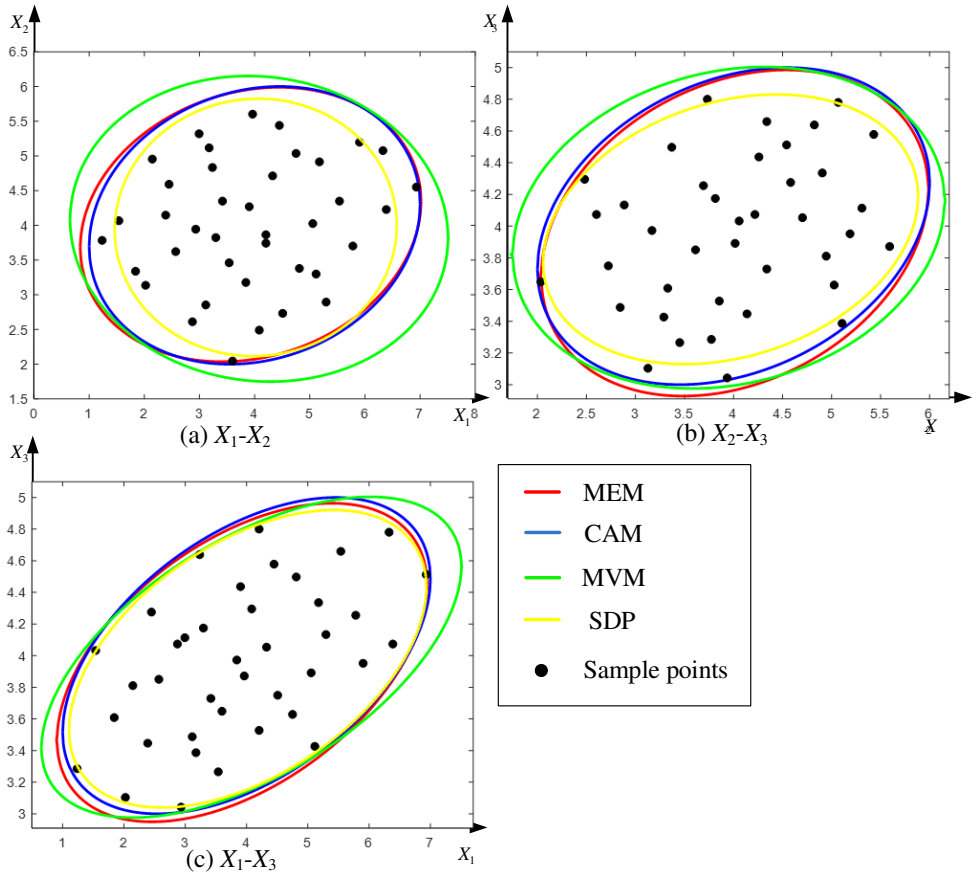

Fig.6 The comparisons of four kinds of ellipsoid models

Table 2 The ellipsoid models by four different methods

MEM:
$$\begin{bmatrix} X_1-3.93 \\ X_2-4.01 \\ X_3-3.96 \end{bmatrix}^{\mathrm{T}} \begin{bmatrix} 1.370\times10^{-1} & -8.813\times10^{-3} & -0.195\times10^{-1} \\ -8.813\times10^{-3} & 0.2749 & -0.1282 \\ -0.195\times10^{-1} & -0.1282 & 1.2883 \end{bmatrix} \begin{bmatrix} X_1-3.93 \\ X_2-4.01 \\ X_3-3.96 \end{bmatrix} \le 1$$

CAM:
$$\begin{bmatrix} X_1-4 \\ X_2-4 \\ X_3-4 \end{bmatrix}^{\mathrm{T}} \begin{bmatrix} 0.145 & -4.520\times10^{-3} & -0.209 \\ -4.520\times10^{-3} & 0.270 & -0.141 \\ -0.209 & -0.141 & 1.382 \end{bmatrix} \begin{bmatrix} X_1-4 \\ X_2-4 \\ X_3-4 \end{bmatrix} \le 1$$

MVM:
$$\begin{bmatrix} X_1-4.08 \\ X_2-3.95 \\ X_3-3.99 \end{bmatrix}^{\mathrm{T}} \begin{bmatrix} 0.130 & 3.17\times10^{-2} & -0.260 \\ 3.17\times10^{-2} & 0.220 & -0.140 \\ -0.260 & -0.140 & 1.520 \end{bmatrix} \begin{bmatrix} X_1-4.08 \\ X_2-3.95 \\ X_3-3.99 \end{bmatrix} \le 1$$

SDP:
$$\begin{bmatrix} X_1-4.02 \\ X_2-3.97 \\ X_3-3.98 \end{bmatrix}^{\mathrm{T}} \begin{bmatrix} 0.153 & -3.84\times10^{-3} & -0.228 \\ -3.84\times10^{-3} & 0.291 & -0.160 \\ -0.228 & -0.160 & 1.47 \end{bmatrix} \begin{bmatrix} X_1-4.02 \\ X_2-3.97 \\ X_3-3.98 \end{bmatrix} \le 1$$

In addition, in order to compare the hyper-volumes of the ellipsoids by four modeling methods, the volume indexes defined by the products of the three half lengths of ellipsoidal axes are calculated,

namely the minimum volume, which are equal to $\prod_{i=1}^{3}\lambda_i^G = 5.33$, $\prod_{i=1}^{3}\lambda_i^J = 5.05$, $\prod_{i=1}^{3}\lambda_i^M = 5.96$ and $\prod_{i=1}^{3}\lambda_i^S = 4.66$. Herein, the superscripts *G*, *J*, *M* and *S* represent the MEM, CAM, MVM and SDP, respectively. The results indicate that the hyper-volumes by MEM is larger than that by CAM and SDP, but smaller than that by MVM. However, as above-mentioned the CAM is an approximate method, and there exists a situation that a very few of samples may be outside of the constructed ellipsoid model. However, the proposed MEM can ensure that all the samples can be completely surrounded.

5.2 Numerical example 2

The bivariate uncertain variables $\mathbf{X}=[X_1, X_2]^{\mathrm{T}}$ are considered in the second example, and the system response function is defined as,

$$y = 0.1*\left(X_1 \sin\left(\omega t\right) - 10X_2 \cos\left(\omega t\right)\right),\ \omega = \frac{\pi}{180} \tag{35}$$

where *t* and ω denote the time and angular frequency.

Through the scatter plot of the 60 samples as shown in Fig. 7, it can be clearly found that the samples have two distinct discrete multimodal and the values of samples are listed in Appendix. Therefore, in order to more accurately and reasonably measure the uncertainty of variable samples, the non-intersecting multi-MEM can be adopted. The optimal parameters of multi-ellipsoid are calculated by MLE and listed in Table 3. Then, with the estimation of the optimal parameter and the normalization process, the following multi-MEM for the samples of uncertain variables can be constructed,

$$\begin{cases} \begin{bmatrix} X_1 - 2.03 \\ X_2 - 2.98 \end{bmatrix}^{\mathrm{T}} \begin{bmatrix} 2.4269 & 1.9433 \\ 1.9433 & 2.7233 \end{bmatrix} \begin{bmatrix} X_1 - 2.03 \\ X_2 - 2.98 \end{bmatrix} \le 1 \\ \begin{bmatrix} X_1 - 3.91 \\ X_2 - 4.95 \end{bmatrix}^{\mathrm{T}} \begin{bmatrix} 2.7599 & -2.2567 \\ -2.2567 & 2.8456 \end{bmatrix} \begin{bmatrix} X_1 - 3.91 \\ X_2 - 4.95 \end{bmatrix} \le 1 \end{cases} \tag{36}$$

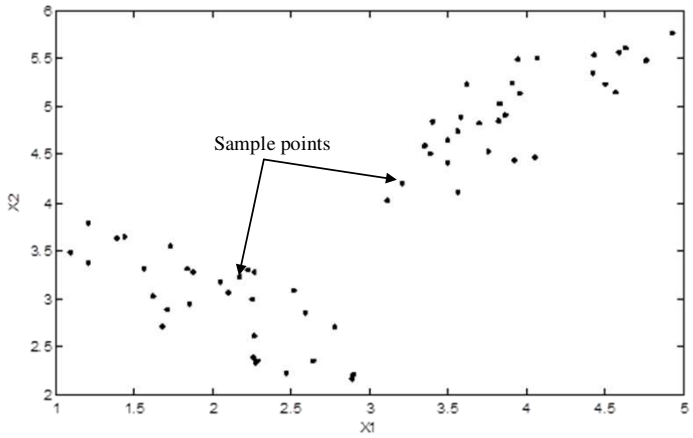

Fig.7 Scatter plot of the samples in example 2

Table 3 The optimal parameters of multi-ellipsoid in example 2

Weighted ratios:	$\alpha = [0.4998,\ 0.5002]^{\mathrm{T}}$
Mean values:	$\boldsymbol{\mu}_1 = [2.03,\ 2.98]^{\mathrm{T}},\ \boldsymbol{\mu}_2 = [3.91,\ 4.95]^{\mathrm{T}}$
Covariance matrices:	$\boldsymbol{\Sigma}_1 = \begin{bmatrix} 0.2324 & 0.1843 \\ 0.1843 & 0.2254 \end{bmatrix},\ \boldsymbol{\Sigma}_2 = \begin{bmatrix} 0.2444 & -0.1744 \\ -0.1744 & 0.2178 \end{bmatrix}$
Scale ratios:	$R_1^2 = 3.93,\ R_2^2 = 4.43$

By comparison, the CAM and MVM for the samples are constructed as Eq. (37), and the compared results are shown in Fig. 8. Obviously, as the distribution and clustering phenomenon of the samples are not considered in CAM and MVM, they only provide more conservative single ellipsoids and contain the blind regions without any samples.

$$\begin{cases} \text{CAM}: \begin{bmatrix} X_1 - 3 \\ X_2 - 4 \end{bmatrix}^{\mathrm{T}} \begin{bmatrix} 0.3504 & -0.1927 \\ -0.1927 & 0.3243 \end{bmatrix} \begin{bmatrix} X_1 - 3 \\ X_2 - 4 \end{bmatrix} \le 1 \\ \text{MVM}: \begin{bmatrix} X_1 - 3.0067 \\ X_2 - 3.9049 \end{bmatrix}^{\mathrm{T}} \begin{bmatrix} 0.3442 & -0.2113 \\ -0.2113 & 0.3635 \end{bmatrix} \begin{bmatrix} X_1 - 3.0067 \\ X_2 - 3.9049 \end{bmatrix} \le 1 \end{cases} \tag{37}$$

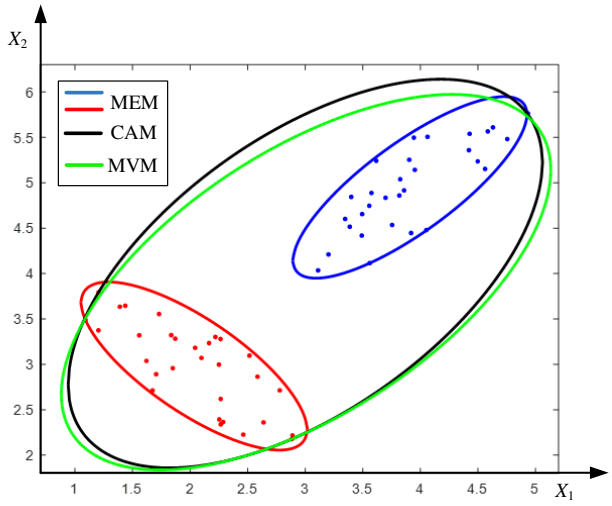

Fig.8 The projections of the ellipsoid models for example 2

Based on the characteristic matrices of multi-MEM, CAM and MVM, the minimum volumes are equal to $\sum_{j=1}^{2}\prod_{i=1}^{2} r_{ij}^{G} = 1.1960$, $\prod_{i=1}^{2} r_i^{J} = 3.6156$ and $\prod_{i=1}^{2} r_i^{M} = 3.6944$. These results quantitatively evaluate the volumes of the three methods and also indicate that the proposed MEM can provide more compact ellipsoid bounds for the uncertainty measurement of the samples with multimodal. Furthermore, the system response bounds under uncertain variables are calculated by using the uncertainty propagation methods of PMA and MCS with 10^6 samples, and the results are shown in Fig. 9. It can be found that the upper and lower bounds of system uncertain response under MEM are very closed to those by MCS, while the response bounds under CAM and MVM are more inaccurate and wide. This illustrates again that the proposed MEM is more suitable to measure uncertainties than CAM and MVM when the samples of uncertain variables display the phenomenon of the obvious multimodal.

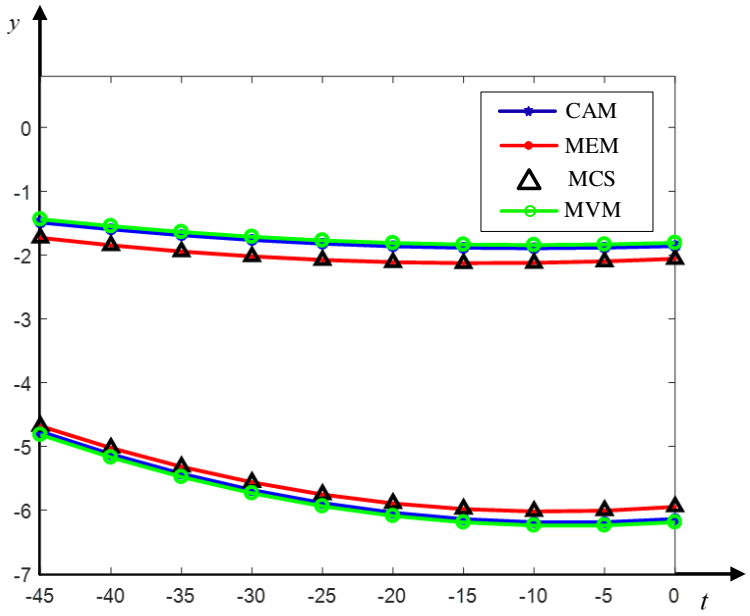

Fig.9 Uncertainty propagation results for example 2

5.3 Numerical example 3

Another bivariate input variables $\mathbf{X}=[X_1, X_2]^{\mathrm{T}}$ are considered in this example, and the system response function is given as

$$y = \mathrm{K}\left(10X_1 - 2X_2\right) \tag{38}$$

where the K denotes the coefficient. The uncertain responses will be analyzed under different K. The samples of uncertain parameter are listed in Appendix**.**

Through the scatter plot of the samples shown in Fig.10**,** it can be found that the samples have two distinct overlap sets. Therefore, we can adopt the intersecting MEM of the type II to measure the uncertainty of variable samples.

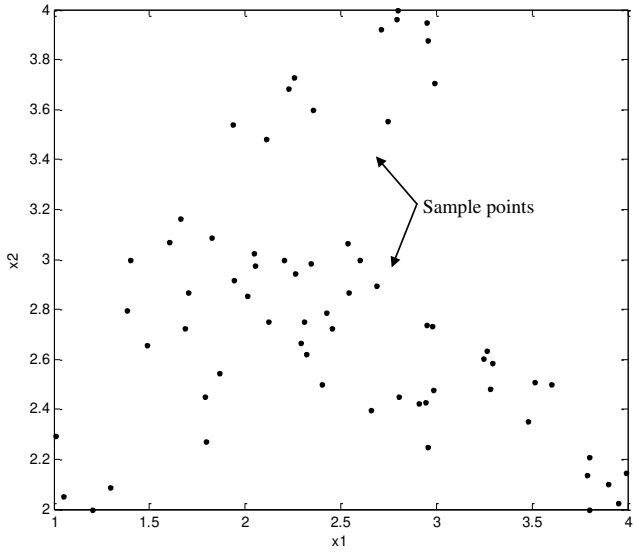

Fig.10 Scatter plot of uncertain variables in example 3

The optimal parameters for the construction of multi-ellipsoid are calculated by GMM and MLE and listed in Table 4.

Table 4 The optimal parameters of multi-ellipsoid in example 3

Weighted averages:	$\alpha = [0.4568; 0.5432]$
Mean values:	$\boldsymbol{\mu}_1 = [2.0467; 3.0880]; \boldsymbol{\mu}_2 = [2.8858; 2.5798]$
Covariance matrixes:	$\boldsymbol{\Sigma}_1 = \begin{bmatrix} 0.3335 & 0.3042 \\ 0.3042 & 0.3820 \end{bmatrix}; \boldsymbol{\Sigma}_2 = \begin{bmatrix} 0.4254 & -0.1627 \\ -0.1627 & 0.0900 \end{bmatrix}$
Scale ratios:	$R_1^2 = 5.115; R_2^2 = 3.871$

Then, by the normalization of scale ratio, the MEM for uncertainty measurement in this example is built as Eq. (39) and shown in Fig.11,

$$\begin{cases} \begin{bmatrix} X_1 - 2.06 \\ X_2 - 3.03 \end{bmatrix}^{\mathrm{T}} \begin{bmatrix} 1.9527 & -1.5162 \\ -1.5162 & 1.8492 \end{bmatrix} \begin{bmatrix} X_1 - 2.06 \\ X_2 - 3.03 \end{bmatrix} \le 1 \\ \begin{bmatrix} X_1 - 3.07 \\ X_2 - 2.43 \end{bmatrix}^{\mathrm{T}} \begin{bmatrix} 3.1797 & 6.4725 \\ 6.4725 & 19.4601 \end{bmatrix} \begin{bmatrix} X_1 - 3.07 \\ X_2 - 2.43 \end{bmatrix} \le 1 \end{cases} \tag{39}$$

By comparison, the constructed CAM and MVM are represented as Eq. (40) and also shown in Fig.11. In view of this, for the samples of uncertain variables with two intersecting sets, the proposed MEM can reasonably and effectively model this kind of uncertainty. However, the CAM and MVM are more conservative and has not the ability to describe internal structure of uncertain samples in detail.

$$\begin{cases} \text{CAM}: \begin{bmatrix} X_1-2.5 \\ X_2-3 \end{bmatrix}^{\mathrm{T}} \begin{bmatrix} 0.3412 & 0.0047 \\ 0.0047 & 0.5397 \end{bmatrix} \begin{bmatrix} X_1-2.5 \\ X_2-3 \end{bmatrix} \le 1 \\ \text{MVM}: \begin{bmatrix} X_1-2.59 \\ X_2-2.69 \end{bmatrix}^{\mathrm{T}} \begin{bmatrix} 0.3615 & -0.0519 \\ -0.0519 & 0.6039 \end{bmatrix} \begin{bmatrix} X_1-2.59 \\ X_2-2.69 \end{bmatrix} \le 1 \end{cases} \tag{40}$$

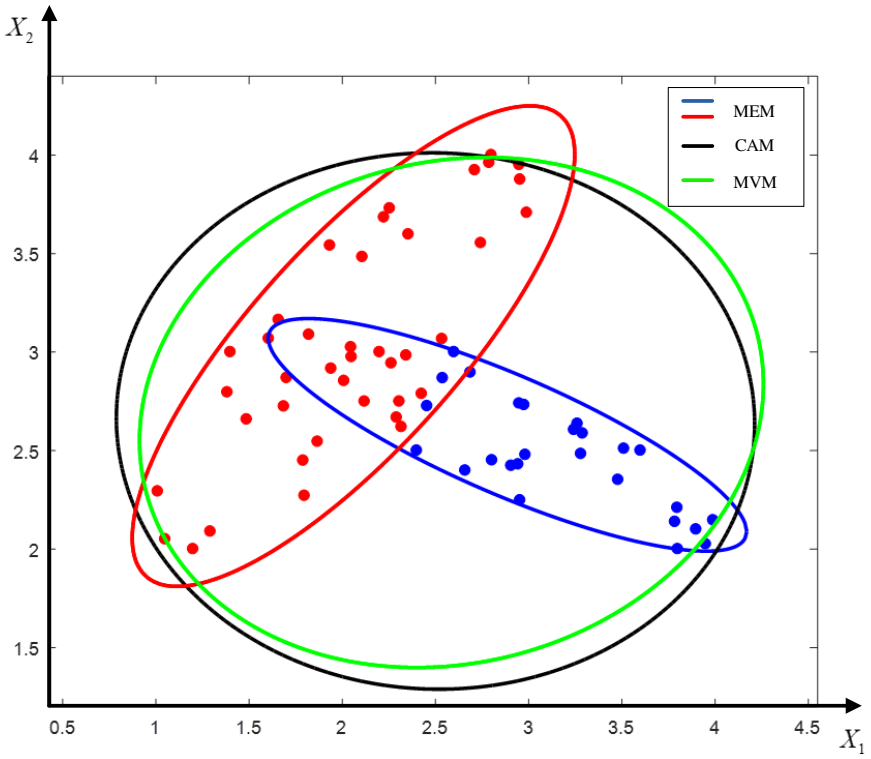

Fig.11 The projections of three ellipsoid models for example 3

Based on the characteristic matrices of MEM, CAM and MVM, the minimum volume are equal to $\sum_{j=1}^{2}\prod_{i=1}^{2} r_i^{\mathrm{G}} = 1.127$, $\prod_{i=1}^{2} r_i^{\mathrm{J}} = 1.2768$ and $\prod_{i=1}^{2} r_i^{\mathrm{M}} = 1.301$, which indicates that MEM can provide a more compact model to measure the variable uncertainties. It should be noted that in order to calculate volume index of MEM, the overlap region of the two component ellipsoids has been counted twice. Nevertheless, the total volume index of MEM is still much smaller than that of CAM and MVM. Then, the system response bounds are computed by using PMA and MCS with 10^6 samples, and the results are shown in Fig.12. It also can be found that for different system coefficient, the propagated uncertain responses under MEM are all almost close to MCS, and more accurate than those under CAM and MVM.

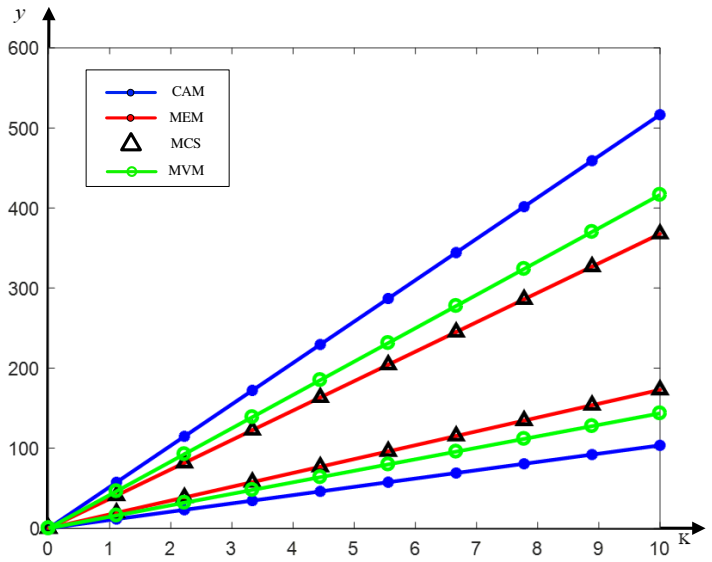

Fig.12 Uncertainty propagation results for example 3

5.4 Engineering application

The thin-walled beam connected by point-welding is a major structure of vehicle body for load bearing and energy absorption. The crashworthiness performance is an important consideration for its design and manufacture. In Fig. 13, the closed-hat beam (Jiang et al. 2007c) is impacted on a rigid wall with the initial velocity of 10m/s. The beam contains a hat beam and a web plate. The web plate is connected by some uniformly distributed point-welding points along the two rims of the hat beam. The material properties of the beam are Young's modulus $E=2.0\times10^5\text{MPa}$, density $\rho=7.85\times10^{-6}\,\text{Kg/mm}^3$, yield stress $\sigma_s=310\text{MPa}$ and tangent modulus $E_t=763\text{MPa}$, respectively. Considering the manufacturing and measuring errors, the plate thickness t, the round radius r, the dimensions L_1, L_2 and L_3 are treated as uncertain parameters. The marginal intervals of the five uncertain parameters are $L_1^{\text{I}}=[16,\ 20]\text{mm}$, $L_2^{\text{I}}=[65,\ 75]\text{mm}$, $L_3^{\text{I}}=[55,\ 65]\text{mm}$, $t^{\text{I}}=[1,\ 2]\text{mm}$ and $r^{\text{I}}=[3,\ 5]\text{mm}$, respectively.

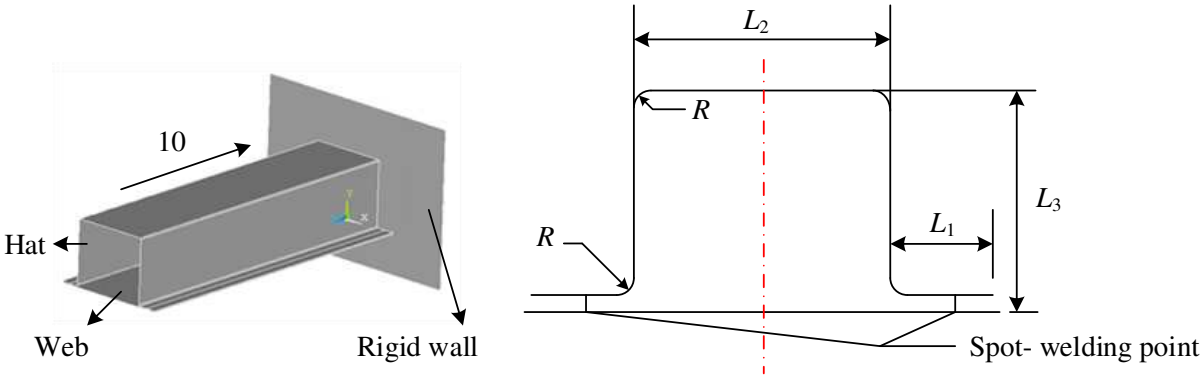

Fig.13 A closed-hat beam impacting on a rigid wall

We assume that the samples have two clusters and based on GMM and MEM, the values of the samples are listed in Appendix, and the optimal parameters for modeling the multi-ellipsoid are estimated and listed in Table 5. Therefore, we can construct the normalized MEM as follows,

$$\begin{cases} \begin{bmatrix} t-1.25 \\ r-3.5 \\ l_1-17 \\ l_2-67.5 \\ l_3-57.5 \end{bmatrix}^{\mathrm{T}} \begin{bmatrix} 21.85 & -8.31 & 0 & 0 & 0 \\ -8.31 & 3.49 & 0 & 0 & 0 \\ 0 & 0 & 0.046 & -0.0047 & -0.0047 \\ 0 & 0 & -0.0047 & 0.0031 & -4.33\text{e-}4 \\ 0 & 0 & -0.0047 & -4.33\text{e-}4 & 0.0068 \end{bmatrix} \begin{bmatrix} t-1.25 \\ r-3.5 \\ l_1-17 \\ l_2-67.5 \\ l_3-57.5 \end{bmatrix} \le 1 \\ \begin{bmatrix} t-1.75 \\ r-4.5 \\ l_1-19 \\ l_2-72.5 \\ l_3-62.5 \end{bmatrix}^{\mathrm{T}} \begin{bmatrix} 22.70 & -9.17 & 0 & 0 & 0 \\ -9.17 & 4.05 & 0 & 0 & 0 \\ 0 & 0 & 0.044 & -0.0035 & -0.0035 \\ 0 & 0 & -0.0035 & 0.0029 & -3.75\text{e-}4 \\ 0 & 0 & -0.0035 & -3.75\text{e-}4 & 0.0068 \end{bmatrix} \begin{bmatrix} t-1.75 \\ r-4.5 \\ l_1-19 \\ l_2-72.5 \\ l_3-62.5 \end{bmatrix} \le 1 \end{cases} \tag{41}$$

Table 5 The optimal parameters of multi-ellipsoid in example 3

Weighted averages:	$\alpha = [0.4568,\ 0.5432]^{\mathrm{T}}$
Mean values:	$\boldsymbol{\mu}_1 = [2.0467,\ 3.0880]^{\mathrm{T}},\ \boldsymbol{\mu}_2 = [2.8858,\ 2.5798]^{\mathrm{T}}$
Covariance matrices:	$\boldsymbol{\Sigma}_1 = \begin{bmatrix} 0.3335 & 0.3042 \\ 0.3042 & 0.3820 \end{bmatrix},\ \boldsymbol{\Sigma}_2 = \begin{bmatrix} 0.4254 & -0.1627 \\ -0.1627 & 0.0900 \end{bmatrix}$
Scale ratios:	$\hat{R}_1^2 = 5.115,\ \hat{R}_2^2 = 3.871$

For the thin-walled beam in a vehicle body, the axial impact force is a key index to evaluate the crashworthiness performance, and it is closely related to the occupant security. Thus, the maximal axial impact force is treated as the system performance function. The corresponding FEM model shown in Fig. 14 is built to compute the maximal uncertain axial impact force under the multi-MEM of Eq. (41). Based on the PMA, the uncertain response of axial impact forces can be effectively solved, and its bounds are [15.9032, 48.0221] kN. By comparison, the result of the MCS with 10^5 samples is provided and the bounds are [13.6581, 55.4738]kN. This result shows that the proposed method can obtain a relatively closed propagation result even with insufficient samples.

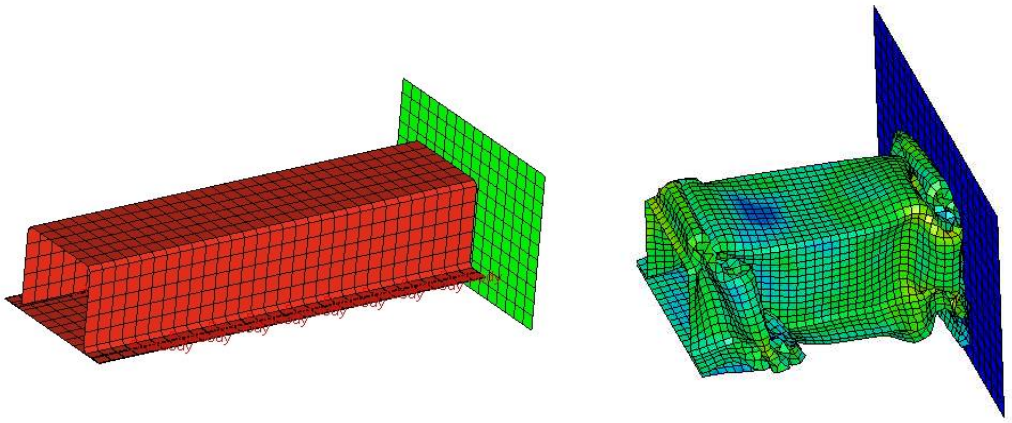

Fig.14 The finite element model of closed-hat beam

6. Conclusions

In this paper, a more generalized non-probabilistic convex model named multimodal ellipsoid model is proposed to reasonably measure the uncertainty of uncertain variables using a single or multimodal samples. The intrinsic distribution of samples is fully considered and the corresponding Gaussian mixture model is constructed. Through the concepts, the samples with one or more similar properties are clustered together, and the principal directions of the samples and characteristic matrix can be appropriately found. Then, the ellipsoidal model of each cluster is modeled by using the elliptical contour features of the Gaussian model. The proposed MEM is a more general uncertainty modeling method, which is suitable for the multi-ellipsoid modeling. In addition, the single-ellipsoid can be regarded as a special case of the multi-ellipsoid. The proposed MEM has many advantages compared with the previous ellipsoid model by the minimum volume optimization method and correlation approximation method. (1) The MEM can provide a suitable modeling process for the non-probabilistic uncertain measurement, which has a rigorous mathematical theoretical foundation. (2) The MEM has a compact structure and the correlation of the MEM is fully based on the relevant samples. (3) The MEM can achieve the multi-ellipsoid modeling, which is impossible for the traditional ellipsoidal convex modelling method. Additionally, a non-probabilistic uncertainty propagation method based on the MEM and PMA is also developed for uncertain structures, in which the MEM is used to quantify the uncertain parameters and the PMA is employed to calculate the bounds of system responses.

Declarations

Availability of data and materials

The datasets used and/or analysed during the current study are available from the corresponding

author on reasonable request.

Competing interests

The authors declare that they have no competing interests

Funding

This work is funded by the National Natural Science Foundation of China (Grant No. 51975199, 11811530285), and the independent research project of State Key Laboratory of Advanced Design and Manufacturing for Vehicle Body, Hunan University (Grant No. 71865010)

Authors' contributions

Jie Liu: Conceptualizaion, Methodology.

Zhongbo Yu: Methodology, Investigation, Writing-Reviewing and Editing

Dequan Zhang: Supervision, Validation

Hao Liu: Writing- Original draft preparation

All authors contributed to writing or correcting the article

Acknowledgements

Not applicable

References

Ben-Haim, Y. (1994). A non-probabilistic concept of reliability. *Structural Safety*, 14(4), 227-245.

Cao, L.X., Liu, J., Han, X., Jiang, C., & Liu, Q.M. (2018). An efficient evidence-based reliability analysis method via piecewise hyperplane approximation of limit state function. *Structural and Multidisciplinary Optimization*, 58(8), 1-13.

Cao, L.X., Liu, J., Jiang, C., Wu, Z.T., & Zhang, Z. (2020). Evidence-based structural uncertainty quantification by dimension reduction decomposition and marginal interval analysis. *Journal of Mechanical Design*, 142 (5).

Celeux, G., & Govaert, G. (1995). Gaussian parsimonious clustering models. *Pattern recognition*, 28(5), 781-793.

Chen, N., Yu, D., Xia, B., & Beer, M. (2016). Uncertainty analysis of a structural–acoustic problem using imprecise probabilities based on p-box representations. *Mechanical Systems and Signal Processing*, 80, 45-57.

Chowdhury, R., & Rao, B.N. (2009). Hybrid high dimensional model representation for

reliability analysis. *Computer Methods in Applied Mechanics and Engineering*, 198(5-8), 753-765.

Degrauwe, D., Lombaert, G., & De Roeck, G. (2010). Improving interval analysis in finite element calculations by means of affine arithmetic. *Computers & Structures*, 88(3-4), 247-254.

Dempster, A.P., Laird, N.M., & Rubin, D.B. (1977). Maximum likelihood from incomplete data via the EM algorithm. *Journal of the royal statistical society*, Series B (methodological), 1-38.

Deng, L., Hinton, G., & Kingsbury, B. (2013). New types of deep neural network learning for speech recognition and related applications: An overview. Proc. Acoustics, Speech and Signal Processing (ICASSP), *IEEE International Conference*, 8599-8603.

Du, X., Sudjianto, A., & Huang, B.. (2005). Reliability-based design with the mixture of random and interval variables. *Journal of Mechanical Design*, 127(6), 1068-1076.

Du, X., & Chen, W.. (2000). A Methodology for managing the effect of uncertainty in simulation-based design. *AIAA Journal*, 38(8), 1471-1485.

Dubois, D., & Prade, H. (1989). Fuzzy sets, probability and measurement. *European Journal of Operational Research*, 40(2),135-154.

Elishakoff, I., & Sarlin, N. (2016). Uncertainty quantification based on pillars of experiment, theory, and computation. Part II: Theory and computation. *Mechanical Systems and Signal Processing*, 74, 54-72.

Ferson, S., Ginzburg, L., Kreinovich, V., Longpré, L., & Aviles, M. (2002). Computing variance for interval data is NP-hard. *ACM SIGACT News*, 33(2), 108-118.

Fraley, C., & Raftery, A.E. (1998). How many clusters? Which clustering method? Answers via model-based cluster analysis. *The Computer Journal*, 41(8), 578-588.

Hofmann, T. (2001). Unsupervised learning by probabilistic latent semantic analysis. *Machine learning*, 42(1-2), 177-196.

Jiang, C., Han, X., Guan, F., & Li, Y.H. (2007a). An uncertain structural optimization method based on nonlinear interval number programming and interval analysis method. *Engineering Structures*, 29(11), 3168-3177.

Jiang, C., Han, X., & Liu, G. (2007b). Optimization of structures with uncertain constraints based on convex model and satisfaction degree of interval. *Computer Methods in Applied Mechanics and Engineering*, 196(49-52), 4791-4800.

Jiang, C., & Han, X.. (2007c). A new uncertain optimization method based on intervals and an

approximation management model. *Computer Modeling in Engineering and Sciences*, 22(2), 97.

Jiang, C., Han, X., Liu, G.R., & Liu, G.P. (2008). A nonlinear interval number programming method for uncertain optimization problems. *European Journal of Operational Research*, 188(1), 1-13.

Jiang, C., Han, X., Lu, G., Liu, J., Zhang, Z., & Bai, Y.C. (2011). Correlation analysis of non-probabilistic convex model and corresponding structural reliability technique. *Computer Methods in Applied Mechanics and Engineering*, 200(33-36), 2528-2546.

Kadapa, C., Dettmer, W., & Perić, D. (2016). A fictitious domain/distributed Lagrange multiplier based fluid–structure interaction scheme with hierarchical B-Spline grids. *Computer Methods in Applied Mechanics and Engineering*, 301, 1-27.

Kang, Z., & Luo, Y. (2009). Non-probabilistic reliability-based topology optimization of geometrically nonlinear structures using convex models. *Computer Methods in Applied Mechanics and Engineering*, 198(41-44), 3228-3238.

Kang, Z., & Zhang, W.. (2016). Construction and application of an ellipsoidal convex model using a semi-definite programming formulation from measured data. *Computer Methods in Applied Mechanics and Engineering*, 300, 461-489.

Kanungo, T., Mount, D.M., Netanyahu, N.S., Silverman, R., & Wu, A. (2002). An efficient k-means clustering algorithm: Analysis and implementation. *IEEE Transactions on Pattern Analysis & Machine Intelligence*, (7), 881-892.

Kass, R.E. (1990). Nonlinear regression analysis and its applications. *Journal of the American Statistical Association*, 85(410), 594-596.

Klir, G.J. (2004). Generalized information theory: aims, results, and open problems. *Reliability Engineering & System Safety*, 85(1-3), 21-38.

Kumar, P., & Yildirim, E.A. (2005). Minimum-volume enclosing ellipsoids and core sets. *Journal of Optimization Theory and Applications*, 126(1), 1-21.

Li, C., Sanchez, R., Zurita, G., Cerrada, M., Cabrera, D., & Vásquez, R. (2016). Gearbox fault diagnosis based on deep random forest fusion of acoustic and vibratory signals. *Mechanical Systems & Signal Processing*, 76, 283-293.

Li, Y., Wang, X., Wang, C., Xu, M., & Wang, L. (2018). Non-probabilistic Bayesian update method for model validation. *Applied Mathematical Modelling*, 58, 388-403.

Liu, J., Sun, X.S., & Han, X. (2015). Dynamic load identification for stochastic structures based on Gegenbauer polynomial approximation and regularization method. *Mechanical Systems and Signal Processing*, 56-57(may), 35-54.

Liu, J., Meng, X.H., & Xu, C. (2018a). Forward and inverse structural uncertainty propagations under stochastic variables with arbitrary probability distributions. *Computer Methods in Applied Mechanics and Engineering*, 342, 287-320.

Liu, J., Cai, H., Jiang, C., Han, X., & Zhang, Z.. (2018b). An interval inverse method based on high dimensional model representation and affine arithmetic. *Applied Mathematical Modelling*, 63, 732-743.

Liu, J., Cao, L., Jiang, C., Ni, B.Y., & Zhang, D. (2020). Parallelotope-formed evidence theory model for quantifying uncertainties with correlation. *Applied Mathematical Modelling*, 77, 32-48.

Liu, J., Liu, H., Jiang, C., Han, X., & Hu, Y.F. (2018c). A new measurement for structural uncertainty propagation based on pseudo-probability distribution. *Applied Mathematical Modelling*, 63, 744-760.

Luo, Y., Kang, Z., Luo, Z., & Li, A. (2009). Continuum topology optimization with non-probabilistic reliability constraints based on multi-ellipsoid convex model. *Structural and Multidisciplinary Optimization*, 39(3), 297-310.

Mcnicholas, P.D., & Murphy, T.B. (2008). Parsimonious Gaussian mixture models. *Statistics and Computing*, 18(3), 285-296.

Meng, X., Liu, J., Cao, L., Yu, Z., & Yang, D. (2020). A general frame for uncertainty propagation under multimodally distributed random variables. *Computer Methods in Applied Mechanics and Engineering*.

Meng, Z., Zhou, H., Li, G., & Yang, D. (2016). A decoupled approach for non-probabilistic reliability-based design optimization. *Computers & Structures*, 175, 65-73.

Meng, Z., Yang, D.X., Zhou, H.L., & Wang, B.P. (2017a). Convergence control of single loop approach for reliability-based design optimization. *Structural and Multidisciplinary Optimization*, 57(3), 1079-1091.

Meng, Z., Li, G., Yang, D., & Zhan, L. (2017b). A new directional stability transformation method of chaos control for first order reliability analysis. *Structural and Multidisciplinary Optimization*, 55(2), 601-612.

Meng, Z., Hu, H., & Zhou, H. (2018). Super parametric convex model and its application for non-probabilistic reliability-based design optimization. *Applied Mathematical Modelling*, 55, 354-370.

Meng, Z., Zhang, Z., & Zhou, H. (2020). A novel experimental data-driven exponential convex model for reliability assessment with uncertain-but-bounded parameters. *Applied Mathematical Modelling*, 77, 773-787.

Moore. R.E. (1979). Methods and applications of interval analysis. *Siam*.

Pouresmaeeli, S., Fazelzadeh, S.A., & Ghavanloo, E. (2018). Uncertainty propagation in vibrational characteristics of functionally graded carbon nanotube-reinforced composite shell panels. *International Journal of Mechanical Science*s, 149(8), 549-558.

Qiu, Z., & Wang, X. (2003). Comparison of dynamic response of structures with uncertain-but-bounded parameters using non-probabilistic interval analysis method and probabilistic approach. *International Journal of Solids and Structures*, 40(20), 5423-5439.

Qiu, Z., & Wang, X. (2005). Two non-probabilistic set-theoretical models for dynamic response and buckling failure measures of bars with unknown-but-bounded initial imperfections. *International Journal of Solids and Structures*, 42(3-4), 1039-1054.

Qiu, Z., & Wang, X. (2005). Parameter perturbation method for dynamic responses of structures with uncertain-but-bounded parameters based on interval analysis. *International Journal of Solids and Structures*, 42(18-19), 4958-4970.

Qiu, Z., Wang, X., & Friswell, M.I. (2005). Eigenvalue bounds of structures with uncertain-but-bounded parameters. *Journal of Sound and Vibratio*n, 282(1-2), 297-312.

Shi, Y., Lu, Z., & Zhou, Y. (2018). Time-dependent safety and sensitivity analysis for structure involving both random and fuzzy inputs. *Structural and Multidisciplinary Optimization*, 58(6), 2655–2675.

Simoen, E., Roeck, G., & Lombaert, G. (2015). Dealing with uncertainty in model updating for damage assessment: A review. *Mechanical Systems and Signal Processin*g, 56, 123-149.

Truong, V., Liu, J., Meng, X., Jiang, C., & Nguyen, T. (2017). Uncertainty Analysis on Vehicle-Bridge System with Correlative Interval Variables Based on Multidimensional Parallelepiped Model. *International Journal of Computational Methods*, 1850030.

Tu, J., Choi, K.K., & Park, Y.. (1999). A new study on reliability-based design optimization.

Journal of Mechanical Design, 121(4), 557-564.

Wang, L., Wang, X., Li, Y., & Hu, J. (2019). A non-probabilistic time-variant reliable control method for structural vibration suppression problems with interval uncertainties. *Mechanical Systems and Signal Processing*, 115, 301-322.

Wang, X., Qiu, Z., & Elishakoff, I. (2008). Non-probabilistic set-theoretic model for structural safety measure. *Acta Mechanica*, 198(1-2), 51-64.

Wei, X., & Du, X.. (2020). Robustness metric for robust design optimization under time-and space-dependent uncertainty through metamodeling. *Journal of Mechanical Design*, 142(3), 031110

Wu, J., Zhang, D., Liu, J., & Han, X. (2019). A moment approach to positioning accuracy reliability analysis for industrial robots. *IEEE Transactions on Reliability*, 99, 1-16

Xiao, Z., Han, X., Jiang, C., & Yang, G.. (2016). An efficient uncertainty propagation method for parameterized probability boxes. *Acta Mechanica*, 227(3), 633-649.

Youn, B.D., & Choi, K.K. (2004). An investigation of nonlinearity of reliability-based design optimization approaches. *Journal of Mechanical Design*, 126(3), 403-411.

Zeng, M., & Zhou, H. (2018). New target performance approach for a super parametric convex model of non-probabilistic reliability-based design optimization. *Computer Methods in Applied Mechanics and Engineering*, 339, 644-662.

Zhang, D., Han, X., & Jiang, C. (2017). Time-dependent reliability analysis through response surface method. *Journal of Mechanical Design*, 139(4), 041404.

Zhang, D., & Han, X. (2020). Kinematic reliability analysis of robotic manipulator. *Journal of Mechanical Design*, 142(4), 044502

Zhang, Z., Jiang, C., Han, X., & Ruan, X.. (2019). A high-precision probabilistic uncertainty propagation method for problems involving multimodal distributions. *Mechanical Systems and Signal Processing*, 126(1), 21-41.

Zhu, L., Elishakoff, I., & Starnes, Jr J. (1996). Derivation of multi-dimensional ellipsoidal convex model for experimental data. *Mathematical and Computer Modelling*, 24(2), 103-114.

Appendix

Table 1 Samples on the uncertainty for numerical example 1.

Number	X_1	X_2	X_3	Number	X_1	X_2	X_3
1	2.030	3.131	3.101	21	2.939	3.939	3.040
2	6.939	4.545	4.515	22	5.788	3.697	4.253
3	1.545	4.061	4.030	23	3.424	4.343	3.727
4	3.848	3.172	3.970	24	3.970	5.596	3.869
5	1.848	3.333	3.606	25	3.000	5.313	4.111
6	2.455	4.586	4.273	26	3.121	2.848	3.485
7	4.818	3.374	4.495	27	5.909	5.192	3.949
8	5.545	4.343	4.657	28	4.333	4.707	4.051
9	3.182	5.111	3.384	29	5.182	4.909	4.333
10	2.152	4.949	3.808	30	4.212	3.737	4.798
11	2.576	3.616	3.848	31	5.121	3.293	3.424
12	3.242	4.828	4.636	32	4.455	5.434	4.576
13	4.212	3.859	3.525	33	3.545	3.455	3.263
14	6.333	5.071	4.778	34	4.758	5.030	3.626
15	4.515	2.727	3.747	35	6.394	4.222	4.071
16	3.909	4.263	4.434	36	1.242	3.778	3.283
17	5.303	2.889	4.131	37	3.606	2.040	3.646
18	3.303	3.818	4.172	38	4.091	2.485	4.293
19	5.061	4.020	3.889	39	2.879	2.606	4.071
20	2.394	4.141	3.444				

Table 2 Samples on the uncertainty for numerical example 2.

Number	X_1	X_2	Number	X_1	X_2
1	2.219399	3.302164	31	4.561986	5.152379
2	2.098374	3.070420	32	3.919348	4.447051
3	1.848857	2.957823	33	4.585504	5.565339
4	2.883305	2.177448	34	3.617155	5.242016
5	2.265046	2.618665	35	4.923524	5.769563
6	2.253232	2.392929	36	3.386686	4.515868
7	2.585320	2.863861	37	4.630296	5.609843
8	2.637891	2.359759	38	3.82427	5.039146
9	1.203835	3.374412	39	3.555722	4.746409
10	2.043340	3.182734	40	4.062128	5.506304
11	1.730330	3.554200	41	4.427443	5.538891
12	2.888488	2.218334	42	3.49437	4.654342
13	2.164607	3.234345	43	3.559939	4.114994
14	1.704952	2.891498	44	3.490927	4.418100
15	2.265823	2.339422	45	3.697514	4.834546
16	1.389795	3.634274	46	4.051388	4.479216
17	2.515282	3.096378	47	3.754507	4.534968

18	1.871032	3.282757	48	3.858271	4.916167
19	1.558403	3.319817	49	3.903247	5.253065
20	1.620956	3.037727	50	4.421196	5.359086
21	2.778897	2.712910	51	3.951404	5.142982
22	2.264103	3.279144	52	3.346107	4.601806
23	1.436786	3.645572	53	3.201740	4.211189
24	1.673714	2.712341	54	3.816983	4.859839
25	1.090868	3.489921	55	4.497481	5.236862
26	1.205242	3.793937	56	3.398991	4.844100
27	2.287038	2.364876	57	3.942939	5.496589
28	2.461811	2.226604	58	3.111521	4.035186
29	1.836134	3.321929	59	3.575249	4.888462
30	2.250109	2.997610	60	4.754638	5.481510

Table 3 Samples on the uncertainty for numerical example 3.

Number	X_1	X_2	Number	X_1	X_2
1	2.047003	3.024703	34	2.659894	2.398765
2	1.383753	2.795835	35	3.280841	2.483089
3	1.867868	2.545125	36	2.975816	2.731471
4	1.790692	2.449206	37	2.539066	2.867686
5	1.292546	2.089197	38	3.797458	2.209633
6	1.605555	3.068134	39	2.803393	2.450792
7	2.788515	3.960966	40	2.426089	2.787934
8	1.658741	3.163222	41	3.898501	2.099965
9	2.119572	2.749110	42	2.982547	2.478538
10	2.22368	3.683864	43	2.292035	2.667583
11	2.743420	3.553580	44	3.261845	2.636314
12	2.107689	3.482994	45	2.943815	2.430078
13	1.821794	3.088321	46	2.906474	2.423041
14	2.254968	3.729583	47	2.317621	2.619858
15	2.535369	3.066336	48	2.455230	2.725981
16	2.263571	2.943001	49	3.289515	2.587145
17	1.686821	2.724282	50	2.343768	2.982947
18	1.940623	2.916136	51	3.243408	2.605289
19	1.487207	2.658422	52	3.511478	2.509604
20	1.934111	3.54114	53	2.687805	2.896319
21	1.797398	2.270627	54	2.306329	2.749182
22	2.355146	3.597509	55	3.479876	2.351604
23	1.701689	2.868603	56	2.953947	2.247553
24	2.711414	3.923396	57	2.949513	2.739245
25	2.954546	3.875804	58	3.785152	2.138332
26	2.800000	4.000000	59	2.200000	3.000000
27	1.200000	2.000000	60	3.800000	2.000000
28	2.600000	3.000000	61	3.600000	2.500000

29	1.400000	3.000000	62	2.400000	2.500000
30	2.989949	3.707107	63	2.010051	2.853553
31	1.010051	2.292893	64	3.989949	2.146447
32	1.050000	2.050000	65	2.050000	2.975000
33	2.950000	3.950000	66	3.950000	2.025000

Table 4 Samples on the uncertainty for numerical example 4.

Number	t	r	l_1	l_2	l_3
1	1.823642	4.645785	18.28857	70.49442	61.41839
2	1.207419	3.354215	16.56333	66.08867	58.58161
3	1.787154	4.645785	19.37397	71.25154	63.58161
4	1.676358	4.354215	18.59142	71.25154	63.58161
5	1.325505	3.645785	17.38391	66.08867	58.58161
6	1.712846	4.354215	18.28857	70.49442	61.41839
7	1.207419	3.354215	16.34701	65.54787	56.41839
8	1.787154	4.645785	18.59142	71.25154	63.58161
9	1.823642	4.645785	19.07112	70.49442	61.41839
10	1.676358	4.354215	19.07112	70.49442	61.41839
11	1.676358	4.354215	18.92888	74.50558	63.58161
12	1.712846	4.354215	19.40858	73.74846	61.41839
13	1.676358	4.354215	18.28857	70.49442	61.41839
14	1.325505	3.645785	16.34701	65.54787	56.41839
15	1.712846	4.354215	19.71143	74.50558	63.58161
16	1.207419	3.354215	16.61609	68.91133	56.41839
17	1.174495	3.354215	16.83241	69.45213	58.58161
18	1.292581	3.645785	16.34701	65.54787	56.41839
19	1.207419	3.354215	16.83241	69.45213	58.58161
20	1.712846	4.354215	18.62603	73.74846	61.41839
21	1.174495	3.354215	17.65299	69.45213	58.58161
22	1.174495	3.354215	16.56333	66.08867	58.58161
23	1.292581	3.645785	16.83241	69.45213	58.58161
24	1.712846	4.354215	19.07112	70.49442	61.41839
25	1.712846	4.354215	19.37397	71.25154	63.58161
26	1.292581	3.645785	16.61609	68.91133	56.41839
27	1.292581	3.645785	17.43667	68.91133	56.41839
28	1.292581	3.645785	17.65299	69.45213	58.58161
29	1.292581	3.645785	16.56333	66.08867	58.58161
30	1.207419	3.354215	17.65299	69.45213	58.58161
31	1.325505	3.645785	17.65299	69.45213	58.58161
32	1.676358	4.354215	19.71143	74.50558	63.58161
33	1.712846	4.354215	18.59142	71.25154	63.58161
34	1.174495	3.354215	17.16759	65.54787	56.41839
35	1.787154	4.645785	18.92888	74.50558	63.58161
36	1.712846	4.354215	18.92888	74.50558	63.58161

37	1.292581	3.645785	17.16759	65.54787	56.41839
38	1.823642	4.645785	19.71143	74.50558	63.58161
39	1.174495	3.354215	17.43667	68.91133	56.41839
40	1.207419	3.354215	17.16759	65.54787	56.41839
41	1.823642	4.645785	18.62603	73.74846	61.41839
42	1.676358	4.354215	19.37397	71.25154	63.58161
43	1.787154	4.645785	19.07112	70.49442	61.41839
44	1.325505	3.645785	17.43667	68.91133	56.41839
45	1.174495	3.354215	16.61609	68.91133	56.41839
46	1.787154	4.645785	18.28857	70.49442	61.41839
47	1.325505	3.645785	16.83241	69.45213	58.58161
48	1.292581	3.645785	17.38391	66.08867	58.58161
49	1.325505	3.645785	17.16759	65.54787	56.41839
50	1.787154	4.645785	19.71143	74.50558	63.58161
51	1.325505	3.645785	16.61609	68.91133	56.41839
52	1.325505	3.645785	16.56333	66.08867	58.58161
53	1.823642	4.645785	19.40858	73.74846	61.41839
54	1.787154	4.645785	19.40858	73.74846	61.41839
55	1.676358	4.354215	18.62603	73.74846	61.41839
56	1.174495	3.354215	17.38391	66.08867	58.58161
57	1.174495	3.354215	16.34701	65.54787	56.41839
58	1.676358	4.354215	19.40858	73.74846	61.41839
59	1.823642	4.645785	19.37397	71.25154	63.58161
60	1.823642	4.645785	18.59142	71.25154	63.58161
61	1.823642	4.645785	18.92888	74.50558	63.58161
62	1.207419	3.354215	17.43667	68.91133	56.41839
63	1.787154	4.645785	18.62603	73.74846	61.41839
64	1.207419	3.354215	17.38391	66.08867	58.58161

Figure captions

Figures

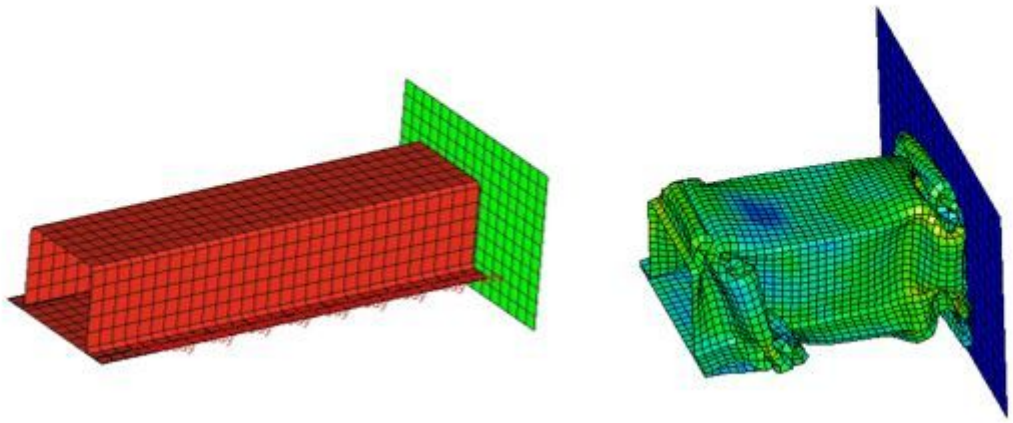

Figure 1

The finite element model of closed-hat beam

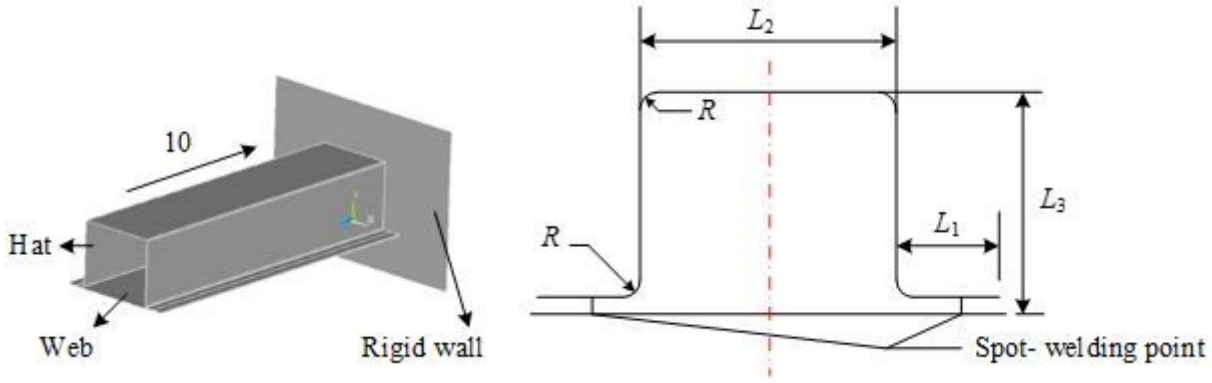

Figure 2

A closed-hat beam impacting on a rigid wall

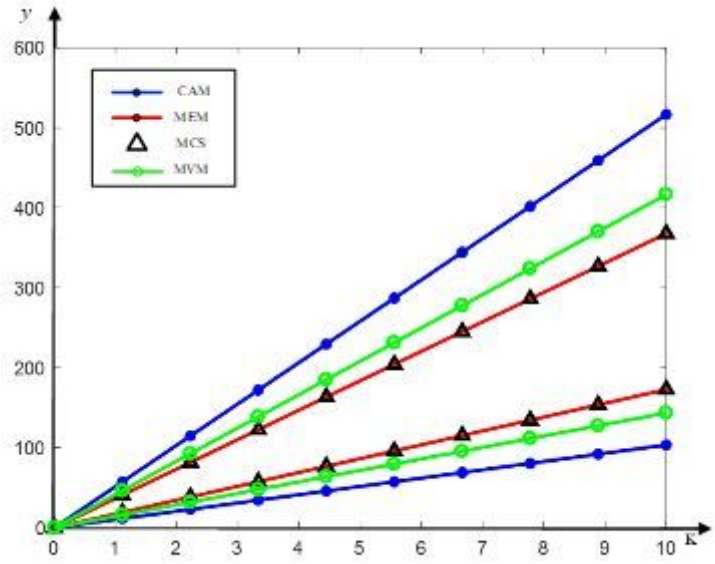

Figure 3

Uncertainty propagation results for example 3

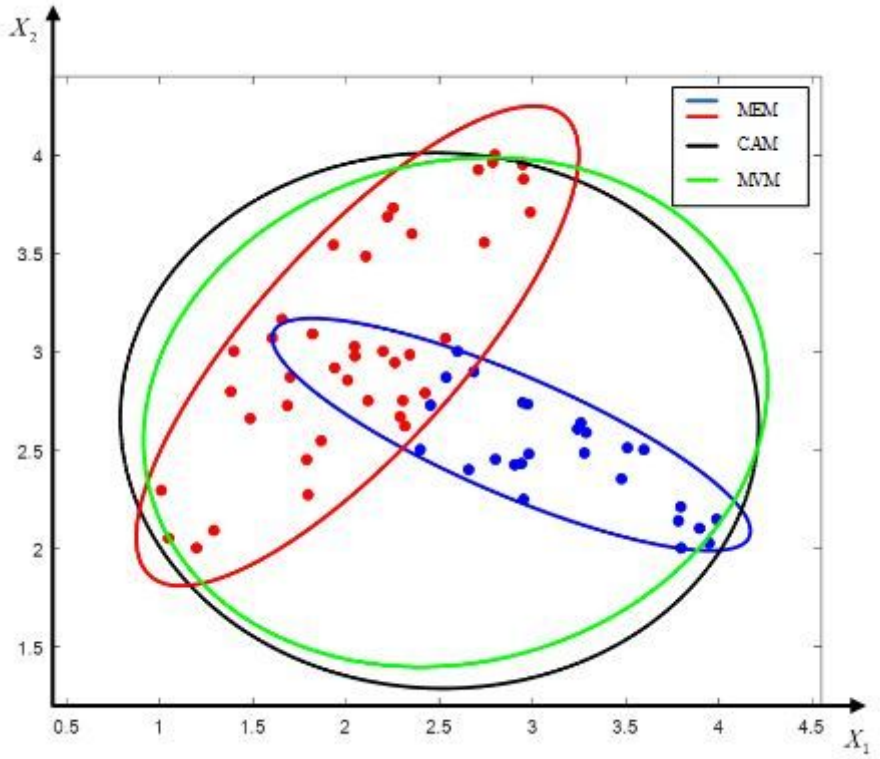

Figure 4

The projections of two ellipsoid models for example 3

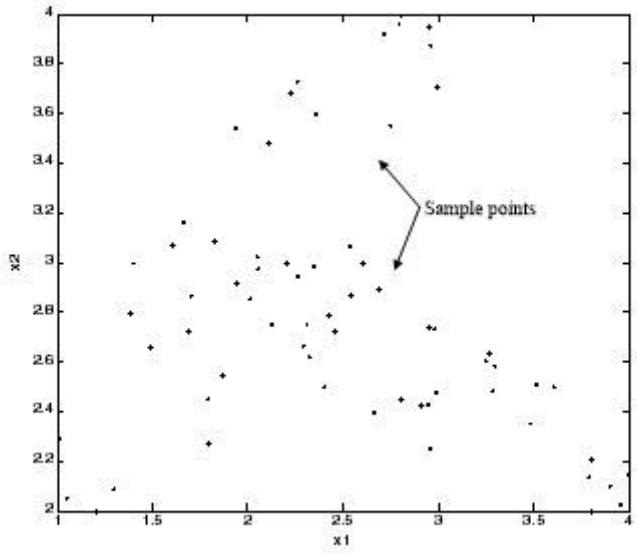

Figure 5

Scatter plot of uncertain variables in example 3

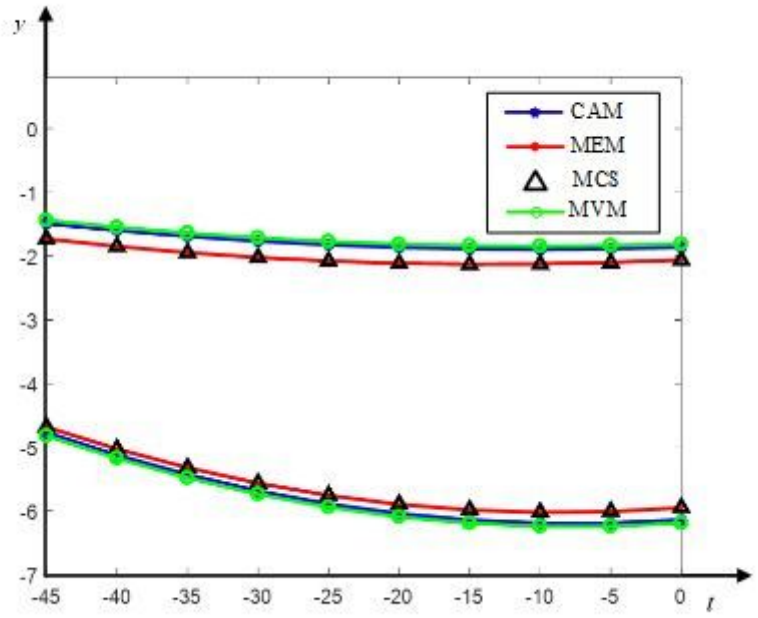

Figure 6

Uncertainty propagation results for example 2

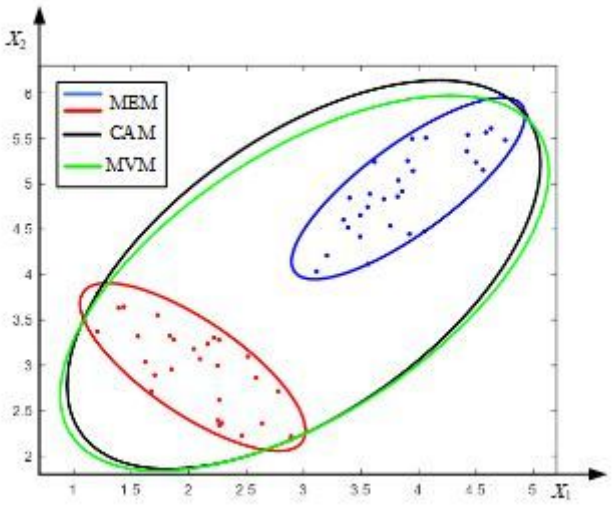

Figure 7

The projections of three ellipsoid models for example 2

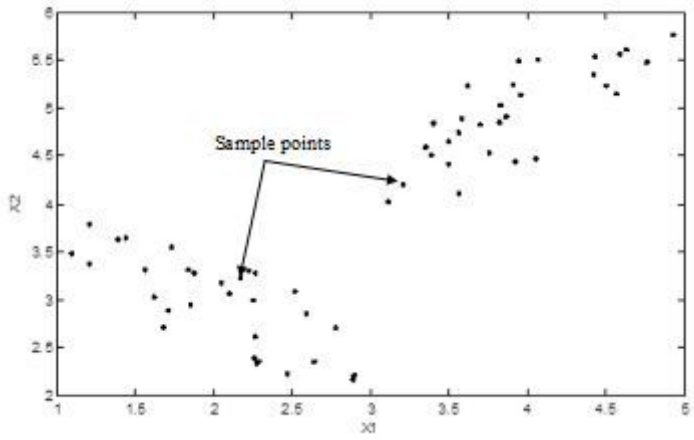

Figure 8

Scatter plot of the samples in example 2

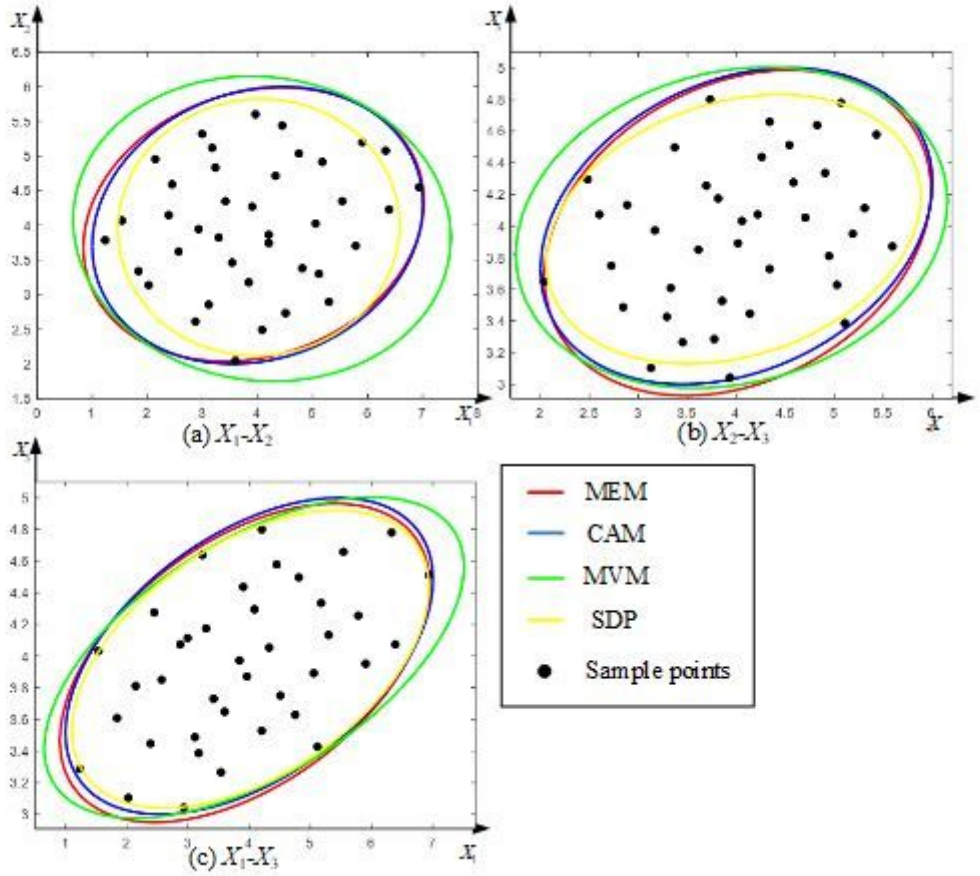

Figure 9

The comparisons of three kinds of ellipsoid models

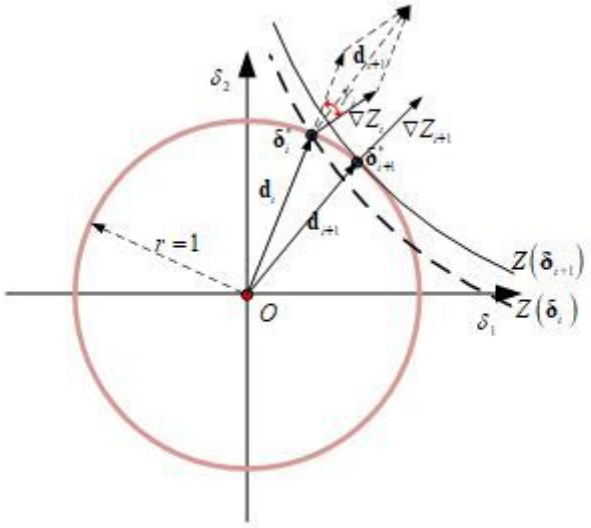

Figure 10

The updating of search direction in space

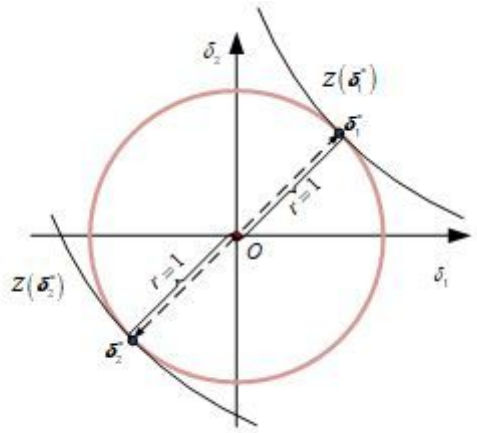

Figure 11

Extreme state of system response in unit sphere space

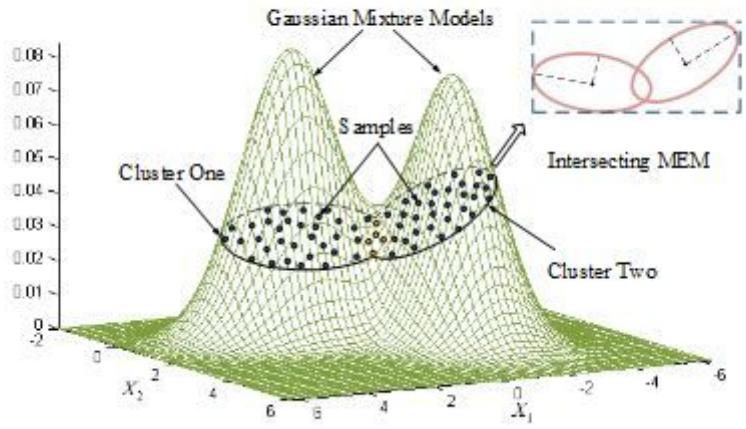

Figure 12

Type II: Intersecting MEM for two dimensional uncertain variables

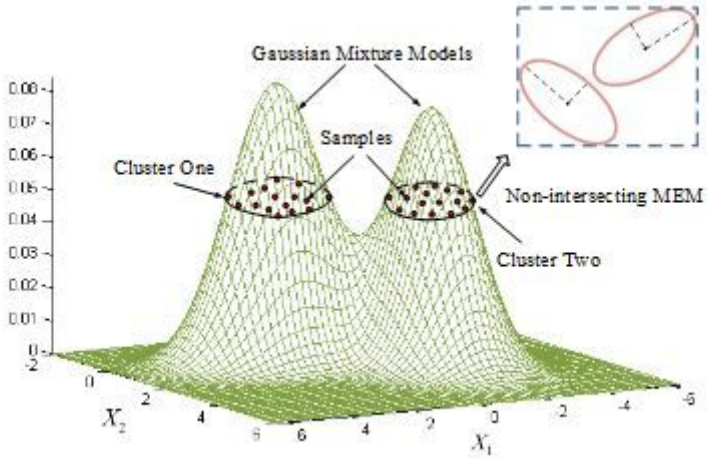

Figure 13

Type I: Non-intersecting MEM for two dimensional uncertain variables

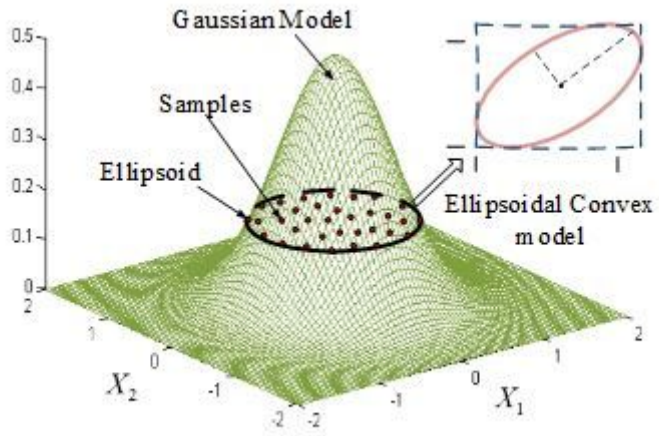

Figure 14

Single-peak distribution for two dimensional uncertain variables